STUDY OF PI-MESONS (PIONS) PRODUCTION IN Pb-Pb COLLISION AT ULTRA-RELATIVISTIC ENERGIES

THIS 02

BY

SAADIA ABBAS

196-FBAS/MSPHY/F13

DEPARTMENT OF PHYSICS
INTERNATIONAL ISLAMIC UNIVERSITY
ISLAMABAD, PAKISTAN

(2015)

i

MS
539.754
SAS

1. Meson - nucleon interactions

2. particles (Nuclear physics)

STUDY OF PI-MESONS (PIONS) PRODUCTION IN Pb-Pb COLLISION AT ULTRA-RELATIVISTIC ENERGIES

By

SAADIA ABBAS

196-FBAS/MSPHY/F13

Supervisor

Dr. Shaista Shahzada

Assistant Professor.

Department of Physics, FBAS, IIUI

Co-Supervisor

Dr. Shakeel Ahmad

Physics Division.

Pakistan Institute of Nuclear Science and Technology (PINSTECH), Islamabad.

DEPARTMENT OF PHYSICS
INTERNATIONAL ISLAMIC UNIVERSITY
ISLAMABAD, PAKISTAN

(2015)

IN THE NAME OF
ALLAH
THE MOST BENEFICENT
THE MERCIFUL

O MY LORD

INCREASE ME IN KNOWLEDGE

(Al QURAN SURA TAHA SECTION 16, 114)

INTERNATIONAL ISLAMIC UNIVERSITY ISLAMABAD

FACULTY OF BASIC AND APPLIED SCIENCES

DEPARTMENT OF PHYSICS

STUDY OF PI-MESONS PRODUCTION IN Pb-Pb COLLISION AT ULTRA-RELATIVISTIC ENERGIES
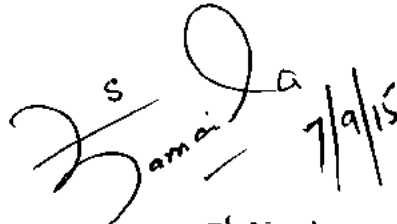
By

SAADIA ABBAS

(Registration No. 196-FBAS/MSPHY/F13)

A thesis submitted to

DEPARTMENT OF PHYSICS

for the award of the degree of

MS Physics

Signature: _____

Chairperson, Department of Physics

Signature: _____

Dean FBAS,IIU,Islamabad

International Islamic University, Islamabad
Faculty of Basic and Applied Sciences
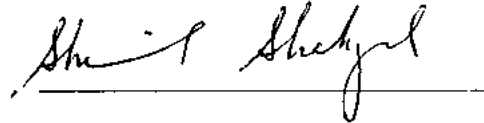# Department of Physics

Approval

It is Certified that the work presented in this thesis entitled "**Study of Pions Production in Pb-Pb Collisions at Ultra-relativistic Energies**" is carried out by **Miss Saadia Abbas**, Registration No. 196-FBAS/MSPHY/F13 under my supervision and that in my opinion, it is fully adequate, in scope and quality, for the award of degree of MS Physics from International Islamic University, Islamabad.

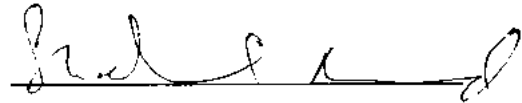## <u>Committee</u>

Supervisor
Dr. Shaista Shahzada
Assistant professor,
Department of Physics (FC), FBAS,
International Islamic University Islamabad.

Co-Supervisor
Dr. Shakeel Ahmad
Physics Division,
Pakistan Institute of Nuclear Science and Technology,
Islamabad.

External Examiner
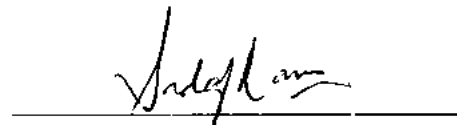**Prof. Dr. Muhammad Tufail**
Head Department of Basic Sciences,
Riphah International University, Islamabad.

Internal Examiner
Dr. Sadaf Jamil Rana
Assistant Professor,
Department of Physics, (FC), FBAS
International Islamic University, Islamabad.

GENERAL PLAGIARISM DECLARATION

1. I hereby declare that I know what plagiarism entails, namely to use another's work and to present it as my own without attributing the sources in the correct way.

2. I know that plagiarism is a punishable offence because it constitutes theft.

3. I understand the plagiarism policy of the Faculty of Basic and Applied Science, International Islamic University Islamabad, Pakistan.

4. I know what the consequences will be, if I plagiaries in any of the assignments for my course.

5. I declare, therefore, that all work presented by me for every aspect of my course, will be my own, and where I have made use of another's work, I will attribute the source in the correct way.

Signature: -/...................................

Name: - Saadia Abbas

196-FBAS/MSPHY/F13

Date: -

DEDICATED

TO

MY AFFECTIONATE PARENTS,
MY HUSBAND AND FATHER IN LAW

A C K N O W L E D G E M E N T S

AUTHOR

(SAADIA ABBAS)

ix

TABLE OF CONTENTS

LIST OF FIGURES

List of Abbreviations

ALICE	A Large Ion Collider Experiment
ATLAS	A Toroidal LHC Apparatus
CERN	European Organization for Nuclear Research
CMS	Compact Muon Solenoid
EMCAL	Electromagnetic Calorimeter
IP	Interaction Point
ITS	Inner Tracking System
LHC	Large Hadron Collider
LHCb	Large Hadron Collider beauty
MC	Monte Carlo
PHOS	Photon Spectrometer
PID	Particle Identification Detection
PMD	Photon Multiplicity Detector
QGP	Quark Gluon Plasma
SDD	Silicon Drift Detectors
SPD	Silicon Pixel Detectors
SSD	Silicon Strip Detectors
TOF	Time of Flight
TPC	Time Projection Chamber
DPM	Dual Parton Model
RQMD	Relativistic Quantum Molecular Dynamics
BME	Boltzmann Master Equation
RHIC	Relativistic Heavy Ion Collider

LIST OF TABLES

ABSTRACT

The main objective of this presented work is to study the production of Pions in Pb-Pb collisions at ultra-relativistic energies as signatures of production of Quark Gluon Plasma (QGP). For this purpose FLUKA (FLUktuierende KAskade) computer code has been used to compute the particle transportation which is a simulation package and is fully integrated for particle physics and Virtual Monte Carlo with main components of offline framework. Virtual Monte Carlo is a set of collaborating classes for primary particle simulation and base classes for fast simulation. In this study, this simulation technique has been employed for ALICE set up of LHC at European Organization for Nuclear Research (CERN, Conseil Européen pour la Recherche Nucléaire), Geneva, Switzerland to study the production of QGP. LHC (Large Hadron Collider) is the largest and most powerful particle accelerator of the world which is up-to-the-minute addition to CERN's accelerator complex and is primarily engaged to test the production of various fundamental particles and to explore the origin of mass. This is offering equivalent platform of computing for analysis at large scale in combination with the PROOF system. The used technique FLUKA, is an all-purpose tool for calculating the particle transport and their interfaces with matter in Accelerator Driven Systems, cosmic rays, neutrino and many more. In this research work the production of pions as result of Pb-Pb interactions at LHC energies has been carried out. This production of pions as signatures of Quark Gluon Plasma has been studied.

CHAPTER 1

INTRODUCTION

Pions belong to the family of hadrons, composed of two quarks and its existence was theoretically predicted by a Japanese scientist H. Yukawa in 1935 [1]. After the prediction these particles were experimentally observed by C.F Powell with his collaborators in 1947 [2]. In attempting to explain the fact that nucleon are bound together due to the strong force in spite of the mutual electrostatic repulsion within them. Yukawa invoked an analogy with electrostatic forces and argues that the forces which hold the nucleon forces are effective at very short distance. By implying the Heisenberg uncertainty principle, he was able to calculate the approximate masses of such particles which came out to be about 200 times of the mass of the electron. These were pions that matched with the prediction of Yukawa. Pions exist in three states $\pi^{\pm}$ mesons and π^0 mesons.

The aim of my research work is to investigate the pions produced and its different decay modes in Pb-Pb collisions at ultra-relativistic energies with the help of Monte Carlo Simulation technique.

1.1 Brief Literature Review and Experimentation

Pions have widely been used to study the induced reactions due to their high interaction ability with the nucleons and transfer of full of their energy to the interacting nucleus. Their production cannot be calculated through first principle of perturbative Quantum Chromo Dynamics (pQCD) and at low collision energies it is not well modelled. It is very significant to study the majority production of particle as a function of both entities firstly the transverse momenta and secondly the particle specie.

To meet the contemporary needs of high energy physics and to test the forces holding together the basic constituents of matter, LHC (Large Hadron Collider) has been built at CERN (European Organization of Nuclear Research) at Swiss-French border. Huge experiments ALICE (A Large Hadron Collider Experiment) and CMS (Compact Muon Solenoid) are being employed to collect the experimental data of p-p collision and Pb-Pb collisions to test the theoretical predictions [3-4]. One of the main purposes for lead-lead interaction is to produce the **Quark-Gluon Plasma** (tiny quantities of matter) and then to study its progression into the kind of matter that makes up the Universe today, since after big bang. This investigation will bring into light the properties of the strong

force. These are the forces that binds quarks into bigger nucleons, for example which binds the protons and neutrons. Heavy-ion collisions provide a unique laboratory for studying very hot and dense matter. This part of the LHC program is investigating matter as it would have been in the first ages of the Embryonic Universe.

There are 82 protons in each lead nucleus. The LHC accelerates each proton to an energy of 3.5 TeV, consequently providing an energy of 287 TeV per beam (3.5×82=287), or a total collision energy of 574 TeV (287×2=574). ALICE (A Large Ion Collider Experiment), ATLAS and CMS (Compact Muon Solenoid) etc. are the major detectors of LHC [5]. The first collisions in the center of the ALICE, ATLAS and CMS collisions was procured after the LHC ended its first run of protons and converted to accelerating lead-ion beams. This lead-ion collision was produced in less than seventy two hours [10]. The pion is identified by numerous independent technique for example exploiting specific energy loss information from the inner tracking system and time projection chamber of the detector.

The decay modes of pions are;

$$\pi^+ \rightarrow \mu^+ + v^+$$

$$\pi^- \rightarrow \mu^- + v^-$$

$$\pi^0 \rightarrow \gamma + \gamma$$

The inverse reactions are also dignified at the same centre of mass energy.

The quark composition of pions, mass and the mean life of π^+, π^-, π^0 is been measured by a wide range of different experiments, since it was established, as given in the following table.

Table 1.1   The quark composition, mass and the mean life of π^+, π^-, π^0

Pion	Quark Composition	Mass (MeV)	Life time (Second)
π^+	$u\bar{d}$	$m_{\pi^+} = (139.56995 \pm 0.0004)$	$\tau_{\pi^+} = (2.603 \pm 0.0005) \times 10^{-8}$
π^-	$d\bar{u}$	$m_{\pi^-} = (139.56995 \pm 0.0004)$	$\tau_{\pi^-} = (2.603 \pm 0.0005) \times 10^{-8}$
π^0	$\dfrac{(\bar{u}u - d\bar{d})}{\sqrt{2}}$	$m_{\pi^0} = (134.9764 \pm 0.0006)$	$\tau_{\pi^0} = (8.4 \pm 0.6) \times 10^{-17}$

The spin of π^+ can be obtained experimentally but there is no straight experimental fortitude of the spin of π^-. Though its spin must be zero as it is antiparticle of π^+. The spin of π^0 is also zero because it is proven theoretically that a system with a spin one cannot decay into two gammas while a system with spin zero can do so. [6-9].

The purpose of this project is to study the pions produced in primary interaction and different decay modes in Pb-Pb collisions at ultra-relativistic energies with the help of Monte Carlo Simulation for ALICE setup, to identify the ensuing pion as the production signals of quark gluon plasma.

CHAPTER 2

LITERATURE PERIODICAL

2.1 THE STANDARD MODEL

Development in the Standard Model of particle physics took the era from mid to the end of 20th century. The Standard Model achieved more reassurance after the discovery of the bottom quark, the top quark and the tau neutrino in 1977, 1995 and 2000 respectively. This Model is sporadically well-thought-out as the "theory of almost everything". Since it has got many achievement in simplifying a wide range of experimental concerns. On the other hand the Standard Model does not clarify the physical connotation of dark mass, dark energy and theory of gravitation as described fully in the theory of general relativity. Some very important properties of neutrino for example: oscillations and their non-zero masses are not correctly accounted in this model. This model is pretty theoretical explanation of interactions of quarks and leptons. Quarks and leptons are the basic constituent of all the matter in the universe. These fundamental particles quarks and leptons are bind together through fundamental forces which are strong, weak and electromagnetic forces. Standard Model is a typical example of QFT (Quantum Field Theory) which discloses a vast variety of concepts in physics for example covering spontaneous symmetry breaking etc. It is used as a basic theory for building several models which include hypothetical particles and symmetries. Some properties of elementary particles estimated by the Standard Model are specified in the table 2.1.

Table 2.1   Classification of atomic particles and their properties e.g. charge, mass etc.

Classification			Name	Symbol	Charge	Mass (MeV/c²)	Life Time (seconds)
Fermions	Leptons		Electron	$e^{\pm}$	$\pm e$	0.5110	x
			Muon	$\mu^{\pm}$	$\pm e$	105.7	2.20×10^{-6}
			Tau	$\tau^{\pm}$	$\pm e$	1784	3.04×10^{-13}
			Neutrino	$\nu_e, \bar{\nu}_e$ $\nu_\mu, \bar{\nu}_\mu$ $\nu_\tau, \bar{\nu}_\tau$	0 0 0	0.320 ± 0.081 eV/c² (sum of 3 flavors)	x x x
	Hadrons	Mesons	Pion	$\pi^{\pm}$ π°	$\pm e$ 0	139.6 135.0	2.60×10^{-8} 0.87×10^{-16}
			Kaon	$K^{\pm}$ $K^{\circ}, (\bar{K}^{\circ})$	$\pm e$ 0	493.7 497.7	1.24×10^{-8} 0.89×10^{-10}
			D meson	$D^{\pm}$ $D^{\circ}, (\bar{D}^{\circ})$	$\pm e$ 0	1869 1865	10.7×10^{-13} 4.3×10^{-13}
		Baryons	Proton	$p, \bar{p}$	$\pm e$	938.3	$> 10^{39}$
			Neutron	$n, \bar{n}$	0	939.6	896
			Lambda	$\Lambda^{\circ}, \bar{\Lambda}^{\circ}$	0	1116	2.63×10^{-10}
			Sigma	$\Sigma^{+}, \bar{\Sigma}^{+}$ $\Sigma^{\circ}, \bar{\Sigma}^{\circ}$ $\Sigma^{-}, \bar{\Sigma}^{-}$	$\pm e$ 0 $\pm e$	1189 1193 1197	0.80×10^{-10} 7.40×10^{-20} 1.48×10^{-10}
			Xi	$\Xi^{\circ}, \bar{\Xi}^{\circ}$ $\Xi^{+}, \bar{\Xi}^{+}$	0 $\pm e$	1315 1321	2.90×10^{-10} 1.64×10^{-10}
			Omega	$\Omega^{-}, \bar{\Omega}^{-}$	$\pm e$	1672	0.82×10^{-10}
Bosons			Photon	γ	0	0	x
			Graviton	2	0	0	Not Yet
			Gluon	1	0	0	Indirectly (not observed singly)
			W^{+}	1	$+1$	80	Yes
			W^{-}	1	-1	80	Yes
			Z^{0}	1	0	91	Yes
			Higgs	H	0	125.06	1.56×10^{-22}

2.2 QUARK-GLUON PLASMA (QGP) SOUP

Making Big Bang soup

Scientist say that in the first millionth of a second aftr the Big Bang, the universe consisted of an unimaginably dense and hot "soup" of quarks and other subatomic part

Quark-gluon plasma

Nuclear particles

Big Bang

Within a ten-thousandth of a second, the universe expanded and cooled to the point that quarks – along with binding particles dubbed gluons – congealed into nuclear particles such as protons and neutrons.

Figure 2.1   Schematic representation of production of QGP.

The physicists arrogate that, when we turn the temperature up to a trillion degrees then at this temperature nuclear material melts into an interesting form of matter which is called a Quark Gluon Plasma (QGP). The universe has been in this state of elemental soup for a microsecond after the Big Bang.

Pressure $+$ Heat (creates pions) $\rightarrow$ Quark-Gluon Plasma
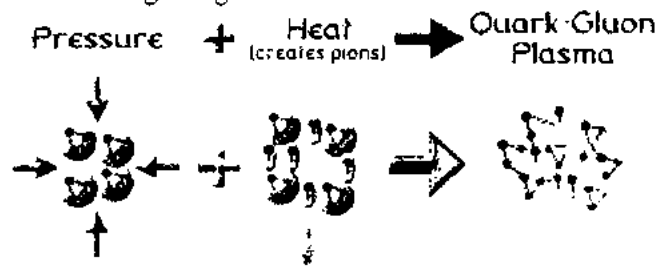
Figure 2.2   Formation process of Quark-Gluon plasma.

Relativistic Heavy-Ion Collider at Brookhaven National Laboratory has the primary purpose of the Re-creating this elemental soup and after collecting data for five years, it appears as if RHIC (Relativistic Heavy Ion Collider) may have succeeded. Then the presumed plasma explodes more violently than predicted [11]. Quark–Gluon Plasma (QGP) contains free quarks and gluons which are among the essential basic constituents of matter. The interaction of quarks and gluons are different from other particles. As they are

separated, they attract each other more strongly at low temperatures. Baryonic matter is composed of Quarks and Gluons [12]. In ordinary matter, quarks are confined where as in the QGP quarks are free to move. The color charge of quarks and gluons is observed in QGP. Outside a finite volume of QGP the color electric field is not displayed, so that Quark-Gluon Plasma must be color-neutral. Therefore, it will have integer electric charge like a nucleus.

2.3   PARTICLE ACCLERATORS

A particle accelerator is a scientific device which is designed to accelerate the electrically charged particles up to tremendously high speeds, to persuade the high energy reactions or to produce high energy radiation [13]. Circular colliders have completely dominated the high energy field in the present situation [14]. The collider LHC is now working in CERN, Geneva, Switzerland.

Table 2.2   Some properties of High-Energy physics accelerators.

Accelerator	Particles	Beam-energy [GeV]	Centre of mass energy [GeV]	Luminosity $[cm^{-2}s^{-1}]$	Remarks
KEK (Japan)	Proton	12	5	-	Fixed target
AGS (Brookhaven)	Proton	33	8	-	Fixed target Polarized p
PS (CERN)	Proton	28 (p) 3.5 (e)	7 -	- -	Fixed target Injector
CESR (Cornell)	e^+, e^-	9	18	10^{32}	Collider
SPS (CERN)	p, e, p, p^-	450 (p), 20(e) 2 x 315	30 (p), - 630	- 3 x10^{30}	F. target, injector Collider
SLC (SLAC)	e^+, e^-		100	6 x10^{30}	Linear Collider
LEP I (CERN)	e^+, e^-	55	110	1.6 x10^{31}	Collider
HERA (DESY)	e, p	30 (e),820 (p)	310	3 x10^{31}	Collider S.C. p-ring
SSC (USA)	p, p	20	0	~ 10^{33}	S.C. collider
LEP II	e^+, e^-	100	200	10^{32}	Collider
LHC (CERN)	p, p	08	16	~ 10^{34}	S.C. collider

CLIC (CERN)	e^+, e^-	01	02	$\sim 10^{33}$	Linear collider

European Organization for Nuclear Research (CERN) has built the world's largest particle accelerator known as LHC. LHC hopefully addresses various basic questions of physics and enhances the understanding of the fundamental laws of nature.

Talking about the structure of LHC then it proves to be a marvelous discovery of science and technology. The LHC is situated in a circular tunnel of 27 kilometers in circumference and 9 kilometers in radius, as deep as 100 meters beneath across the France and Switzerland border near Geneva, Switzerland. Different experimental setups containing of various detection techniques have been arranged in the LHC tunnel and all of them are designed for particular type of investigation. The synchrotron of LHC is designed for the collision of opposed beams of protons up to 7 TeV [15-16]. More than 15,000 scientists and engineers from different laboratories and universities, over 100 countries took part in the construction of LHC [17]. The main purpose of LHC physics plan is proton–proton collisions. However, for short intervals of time, normally one month in a year, heavy-ion interactions are incorporated in this program [18]. Six detectors are located at the intersection points of LHC's tunnel. A Toroidal LHC Apparatus (ATLAS) and Compact Muon Solenoid (CMS) are gigantic setups which are designed to detect the particle ensuing from p-p and Pb-Pb interactions [19]. A Large Ion Collider Experiment (ALICE) and LHCb possess more particular tasks and European Organization for Nuclear Research (CERN) has fabricated the world's largest particle accelerator known as LHC. LHC hopefully addresses various basic questions of physics and enhances the understanding of the fundamental laws of nature. A Large Ion Collider Experiment (ALICE) and LHCb possess more particular tasks and remaining two very small detectors, TOTEM and LHCf are designed for specific research.
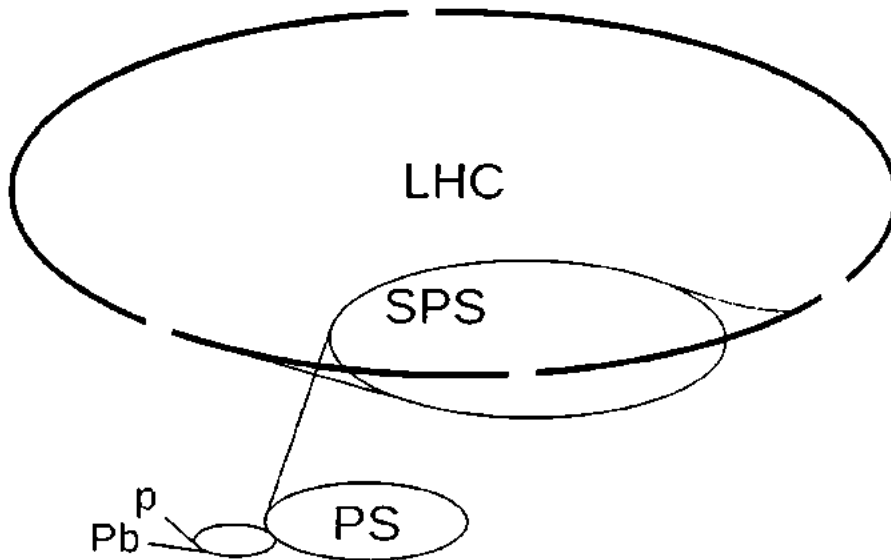
Figure 1.3   Schematic representation of Large Hadron Collider (LHC).

2.4   PROPERTIES OF PI-MESONS (PIONS)

When Yukawa in 1935 tried to find the field theory of nuclear force a lot significant developments occurred in the field of theoretical physics. This attempt was after the Fermi theory that was developed for β-decay [20]. Wolfgang Pauli, in 1930 hypothesized the existence of the neutrino, he was attempting to explain the continuous distribution of energy of the electrons which emits in beta decay. Enrico Fermi by 1934 had established a theory of beta decay to explain the neutrino, for this he imaginarily supposed neutrino to be massless and charge less [21]. Yukawa have used the virtual emission and absorption of electron-neutrino pair between the neutron and proton and this is how, he tried to produce the strong nuclear force between the nucleons. When the charged particles exchange of photons between them electromagnetic forces are generated. Yukawa has considered this analogy of these electromagnetic forces the ground of his concerns. As the exchanged photons are massless this thing have made the range of the Coulomb forces an infinite range of interaction.   Yukawa showed that interchange of considerable quanta between nuclear particles would give growth to a short range force and the range of this short range force is inversely proportional to the mass of the exchanged particles. He found the strength of β-decay coupling is not strong enough to be able to generate the strong nuclear force. Yukawa consequently set forth another notion of transformation of the neutron into the proton, this new idea contains emission of another

10

kinetic energy and rest mass energy which leads to high nuclear excitations. Therefore, even a nucleus having high fission barrier can be subjected to collapse under shower with pions. There are two main characteristics of pion induced fission studies.

i.   The effects of interior agitation on fission prospects, with and without high angular momentum can be evaluated because the reactions of pion with nucleus offer a condition, in which high nuclear excitations are attained.

ii. The pion obliged as an intermediate step particle. For nuclear excitations by projectiles alike to the photons and antiprotons.

By using charged pions of different energies, dimension of fission cross-sections in various targets are made which is an important step to understand behavior of nuclear many body system at high temperatures [25]. Studies of the interaction of the pions have been of great interest for the last many years. Some systematic experiments were carried out for the measurement of parameters such as binary fission cross-sections and angular distributions of track length of the reaction products etc. [26].

Rapid progress have been made in this field with the edifice of accelerators of high energy, at various institutions. These accelerators has powered the development of an age of good measurements with which the accurate values for the particle's mass, it's lifetime, spin and parity etc can be obtained. Quarks are the elementary particles, properties of quarks are given in the table 2.3.

Table 2.3   Classifications and properties of quarks in to different generations i.e. charge and rest mass etc.

Generations	Quarks	Symbol	Rest mass (GeV/c^2)	Electric charge	Strange	Charm	Top	Bottom
1	Up	u	$\leq 3 \times 10^{-3}$	$\frac{2}{3}$	0	0	0	0
	Down	d	$\approx 7 \times 10^{-3}$	$-\frac{1}{3}$	0	0	0	0
2	Charm	c	≈ 0.12	$\frac{2}{3}$	0	1	0	0
	Strange	s	≈ 1.2	$\frac{1}{3}$	-1	0	0	0
3	Top	t	≈ 4.2	$\frac{2}{3}$	0	0	1	0
	Bottom	b	$\approx 175 \pm 5$	$\frac{1}{3}$	0	0	0	-1

2.4.1 PRODUCTION AND DECAY OF PIONS

Pions are also produced by proton (p), antiproton ($\bar{p}$) annihilation and neutron (n), antineutron ($\bar{n}$) annihilation.

$$p + \bar{p} \rightarrow \pi^+ + \pi^- + \pi^\circ \qquad (2.3)$$

$$n + \bar{n} \rightarrow \pi^+ + \pi^- + \pi^\circ + \pi^\circ \qquad (2.4)$$

Pions can also be produced when a nucleon is exposed to γ-ray photon, such as:

$$\gamma + p \rightarrow \pi^+ + n \qquad (2.5)$$

$$\gamma + n \rightarrow \pi^- + p \qquad (2.6)$$

The neutral pions can also produce by bombarding hydrogen (protium and deuterium) with high energy photon.

$$\gamma + p \rightarrow \pi^\circ + p \qquad (2.7)$$

$$\gamma + d \rightarrow \pi^\circ + (n + p) \qquad (2.8)$$

$$\gamma + d \rightarrow \pi^\circ + d \qquad (2.9)$$

Charged pions can also be produced from photons and from heavy ion collisions.

Charged pions are unstable and primarily decay with a half-life ($T_{1/2}$) of about 2.6×10^{-8} second. This decay process is as follows:

$$\pi^+ \rightarrow \mu^+ + \bar{v}_\mu \qquad (2.10)$$

and further $\qquad \mu^+ \rightarrow e^+ + v_e + \bar{v}_e \qquad (2.11)$
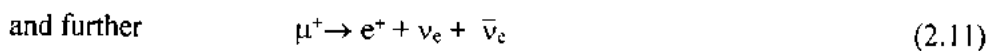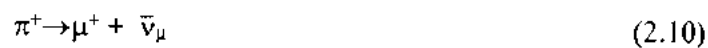
Equation 2.10 shows that the μ^+ (positively charged muon) subsequently decays into a positron and a neutrino pair. Pions may also decay according to the reaction [28]:

$$\pi^+ \to e^+ + \nu_e \tag{2.12}$$

$$\pi^+ \to \mu^+ + \nu_\mu + \gamma \tag{2.13}$$
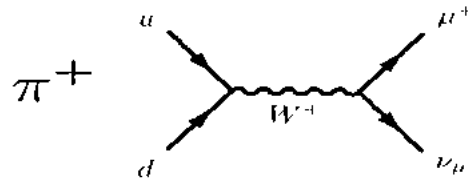
$$\pi^+ \to \pi^\circ + e^+ + \nu_e \tag{2.14}$$

Similarly the possible decay processes with negative pions are as follow [29]:

$$\pi^- \to \mu^- + \bar{\nu}_\mu + \gamma \tag{2.15}$$
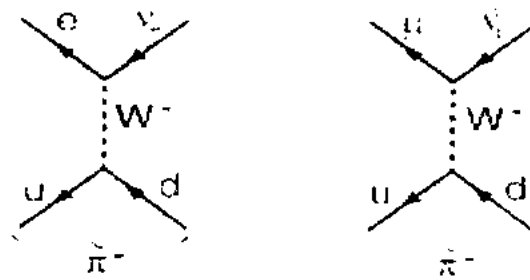
$$\pi^- \to e^- + \nu_e^- \tag{2.16}$$

$$\pi^- \to \pi^\circ + e^- + \bar{\nu}_e \tag{2.17}$$

The most likely decay mode [(Branching Ratio)] of the π° meson is:
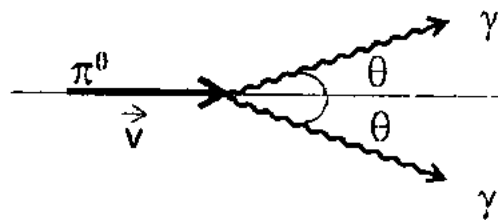
$$\pi^\circ \to \gamma + \gamma \tag{2.18}$$

The mean life of π° is about 0.87×10^{-16} second [30]. π° cannot decay into only one photon because the momentum could not be conserved. In fact, in all these decays at least two particles must be produced in order to conserve momentum.

14

Rare decay modes are also possible for example:

$$\pi^\circ \rightarrow \gamma + e^+ + e^- \qquad (2.19)$$

$$\pi^\circ \rightarrow 2e^+ + 2e^- \qquad (2.20)$$

- The dominant decay mode is $\pi^- \rightarrow \mu^- + \bar{\nu}_\mu + \gamma$ with branching ratio of (99.98770 ± 0.0004) %.

- The spin of π^+ can be persist by using a decay mode $p + p \rightarrow \pi^+ + d$.

- Direct experimental grit of the spin of π^- is not possible, though the spin of π^- must be zero because it is just the antiparticle of π^+.

- The $\pi^\circ \rightarrow \gamma + e^+ + e^-$ mode of π° has branching ratio (1.198 ± 0.032) %.

- π° has spin zero because it is proven theoretically that a system with spin one cannot decay into two gammas while a system with spin zero can decay into two gammas [27].

2.4.3 PION REST MASS ENERGY (THEORETICAL ESTIMATION)

Pion rest mass energy was theoretically estimated and formulated through Yukawa's theory of nuclear force. In each exchange reactions, violation of law of energy conservation takes place and to the extent of uncertainty principle that is:

$$\Delta E \, \Delta t \cong \hbar \qquad (2.21)$$

Whereas:

ΔE = Energy of the pion mass,

Δt = Time between the ejection of pion by one nucleon and its capture by the other nucleon,

$\hbar = h / 2\pi$ and

h = Planck's constant.

Considering the range of nuclear force = 1.5×10^{-13} cm and pion velocity as velocity of light

$$\Delta t = 1.5 \times 10^{-13} / 3 \times 10^{10}$$

$\Delta t = 0.5 \times 10^{-23}$ second.

$\Delta E = h \,/(2\pi \times \Delta t)$

$\Delta E = 6.63 \times 10^{-34}/(2 \times 3.142 \times 0.5 \times 10^{-23})$ Joules

$\Delta E = 6.63 \times 10^{-34}/(2 \times 3.142 \times 0.5 \times 10^{-23} \times 1.6 \times 10^{-19})$ eV

$\Delta E = 131.88$ MeV.

This value of the rest mass energy of pion is close to the measured value i.e. 139.6 MeV ($\pi^{\pm}$) and 135 MeV (π°) [31]. This proves that the exchange particle involved in the nuclear force is π-meson, as predicted by Yukawa's theory.

CHAPTER 3

EXPERIMENTATION AND ADOPTED METHODS

3.1 ENERGY DOMAINS OF HEAVY ION COLLISIONS

The interaction energy regions can be divided into three regimes.

1. INTERMEDIATE ENERGY HEAVY ION REACTIONS
2. RELATIVISTIC ENERGY HEAVY ION REACTIONS
3. ULTRA- RELATIVISTIC ENERGY HEAVY ION REACTIONS

3.1.1 INTERMEDIATE ENERGY HEAVY ION REACTIONS

In this energy region properties of hot nuclear matter can be studied around n_0 which is normal nuclear density. The energy ranges from (10 to 100) A.MeV for corresponding Beam energies. The methods which is applied in this range results in small nuclear fragments.

3.1.2 RELATIVISTIC ENERGY HEAVY ION REACTIONS

In this region energy ranges from 100A MeV to 10A.GeV. In this region mainly the compressibility and other nuclear interaction can be discussed. This is the area where we mostly study the nucleon-nucleon reactions in both ways experimentally as well as theoretically. Few accelerators which are working in this energy domain are SATURN in France, BEVALAC at LBL at Berkeley and the heavy ion accelerator in Dubna.

3.1.3 ULTRA- RELATIVISTIC ENERGY HEAVY ION REACTIONS

The most intriguing question in particle physics is search for Quark gluon Plasma. This energy domain starts from 10A.GeV, which is the most optimistic theoretically estimated range for the foundation of quark-gluon plasma.

This range can be further divide into two regimes:

1   STOPPING REGION
2   TRANSPARENT REGION

3.1.3.1 STOPPING REGION

Where baryons halting from the projectile and the target is fully or partially stopped by each other. This thing forms a fairly opulent baryon matter in the middling of the reaction zone. Experiments done at SPS CERN and AGS at BNL showed that there is complete stopping in reactions up to 60A.GeV. More experiments have showed that with lead beam up to (200 or 800) A.GeV will results in stopping the baryon matter in the Centre of the reaction zone.
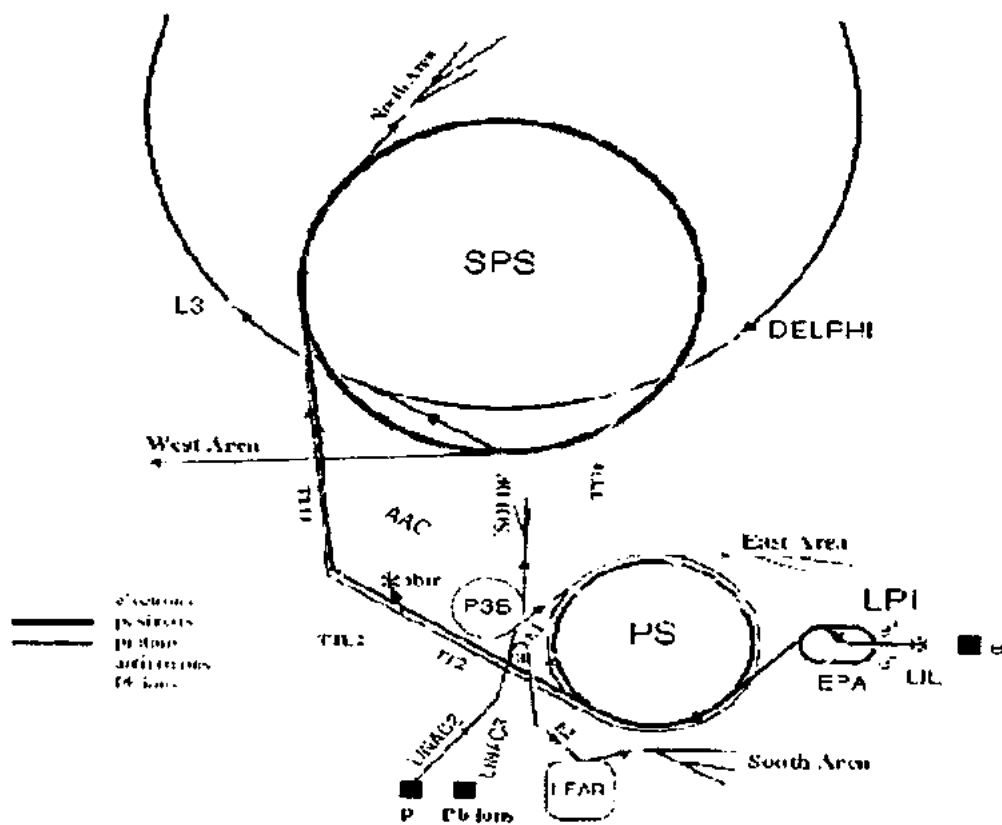
Figure 2.1   The schematic layout of SPS at CERN. Geneva.

3.1.3.2 TRANSPARENT REGION

If in the phase space the target and the projectile are so far apart that the heavy ion collision cannot slow them down completely. The initial baryon charge from the target and the projectile will not slowed completely if we keep on increasing the energy. Due to the initial velocity of the quanta which carry this baryon charge, the middle zone in the reaction will become charge free and energy will be deposit in this region. This large energy density matter in the center region forms a baryon free quark gluon plasma. This baryon free quark gluon plasma is of more interest for theoretical predictions then to the baryon opulent quark gluon plasma. Different studies disclosed that this form of plasma was present in the early universe (high in energy density but low in baryon density), just before the hadrons were found. LHC heavy ion collider at CERN, RHIC at BNL, and the TEVATRON at Fermi lab can be considered as colliders relevant to this energy domain [32-33].

Figure 3.2   The layout of Relativistic Heavy Ion Collider at Brookhaven National Laboratory

3.2 LHC: LARGE HADRON COLLIDER

The world's leading and most dominant particle accelerator is LHC. It is the latest addition to CERN's accelerator complex. It's working scheme and internal structure is been elaborated briefly as follows:

➤ *Working Scheme:*

High-energy particle beams travels at nearby to the speed of light, inside the accelerator, before they are made to collide. These beams travel in contrary directions in separate beam pipes. Both beam pipes are kept at 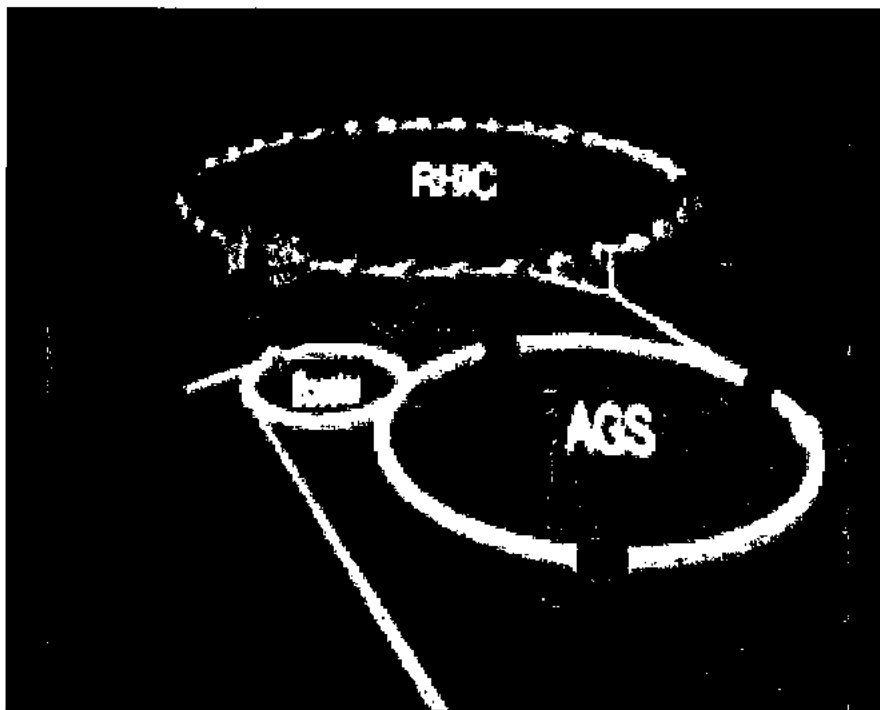ultrahigh vacuum, this ultrahigh vacuum is the vacuum regime characterised by pressures lower than about 10^{-7}Pascal. These beams are directed around the accelerator ring by a strong magnetic field which is maintained by superconducting electromagnets. The particles in the beam are so tiny that colliding them is just like to firing two needles from the distance of 10 kilometres apart with such accuracy that they meet halfway. The beams inside the LHC are made to collide at four places around the accelerator ring. These four locations are known as partial detectors:

i.   ATLAS.
ii. CMS.
iii. ALICE.
iv. LHCb.

➤ *Internal Structure of LHC in Brief:*

The circumference of LHC is 27 km, it is a ring of superconducting magnets. Numerous accelerating structures boost the energy of the particles along the way.The electromagnets are made up of coils of exceptional electric cable. These cables operates in a superconducting state and they conduct electricity efficiently without resistance or loss of energy. These magnets require up to -459.4°F chilling temperature [35], for this reason system of liquid helium, is connected to accelerator for cooling the magnets and other hoard services.
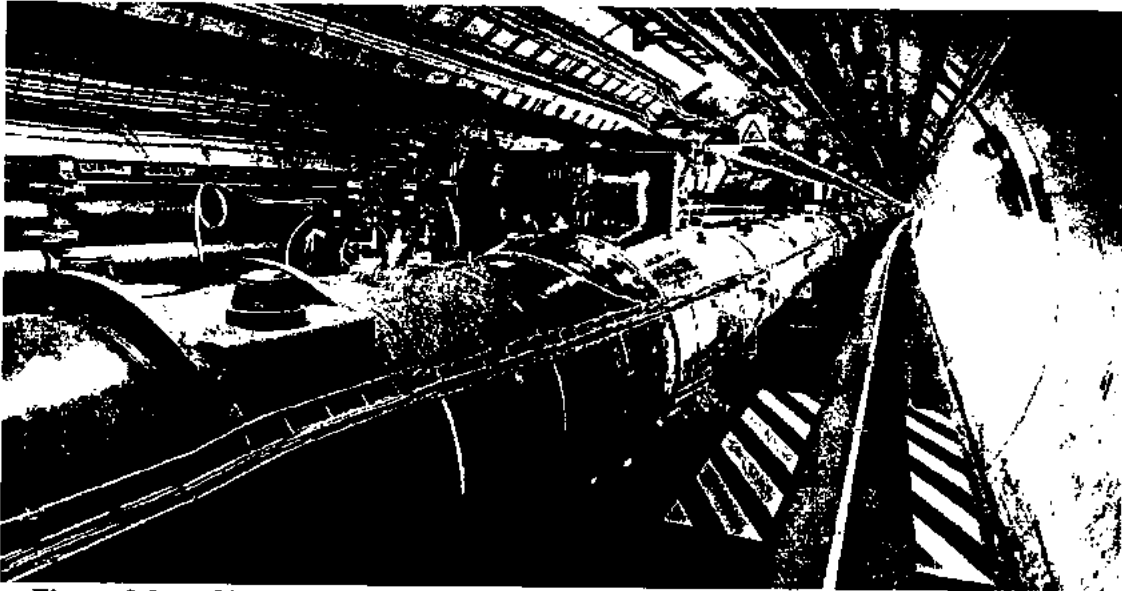
Figure 3.3 Photograph of the Large Hadron Collider, the world's largest and most powerful particle accelerator (Image: CERN)

A lot of magnets of different varieties and sizes are used to through the beams around the accelerator.

1. 1232 dipole magnets which are 15 metres in length bend the beams.

2. Prior to collision, 392 quadrupole magnets which are 5–7 each metres long in length concentrate the beams.

3. A magnet is used to cuddle the particles closer to rise the probabilities of collisions. [34].

3.3 INTRODUCTION TO ALICE

ALICE is particularly used to study heavy ion collisions such as collisions of Pb-Pb nuclei [36-37]. Collisions that befell in LHC the temperature is 100,000 times more than the temperature of the Sun which is such a high temperature that the protons and neutrons decays, and quarks turn out to be free from their bonds with the gluons. All nucleons are composed of quarks, a strong nuclear force holds them together the carrier particles of these nuclear forces are called gluons. The combination of quark and gluon at such a high temperature is called plasma. In this plasma the strong interactions become small, and then it is recognized as the Quark-Gluon Plasma (QGP) [66]. The ALICE experiment is particularly used to study the quark-gluon plasma and to answer the questions like how the vital particles establishes the universe [38]. It is in the search to answers some more fundamental questions such that what will happen if the matter is

21

treated at the heat more than 100,000 times the heat of Sun? What is the reason of 100 times increased weight of neutron and proton then to the quarks from which these are made up of and is it possible that quarks may get free from inside the proton or neutron [39-40].

ALICE is fixated on the study of heavy ion collisions at the LHC and typically used to answer the above questions. To this end there was a need to study the extravagances of this theory at small interaction [42]. On 23 November 2009, the first p-p collisions were observed in ALICE, during the initial commissioning phase of the LHC this collision was observed. Duration of this phenomenon of colliding beams was about one hour for each of its four large experiments [41]. Data acquirement started from 6 December 2009, when the stable beams were declared.

3.3.1 DETECTOR'S STRUCTURE

ALICE detector is used to restore the decay of baryon which are consist of either strange or charm quark. Just like an onion it is well layered It is used to detect different chattels of particles when the particle pass through it [43]. ALICE detector has different parts for example the central part or main barrel, a muon detector. a cosmic detector, The L3 magnet which is used to produce a magnetic field parallel to beam axis and so many other detectors. The Figure 3.4 contains the indication of sub detectors.
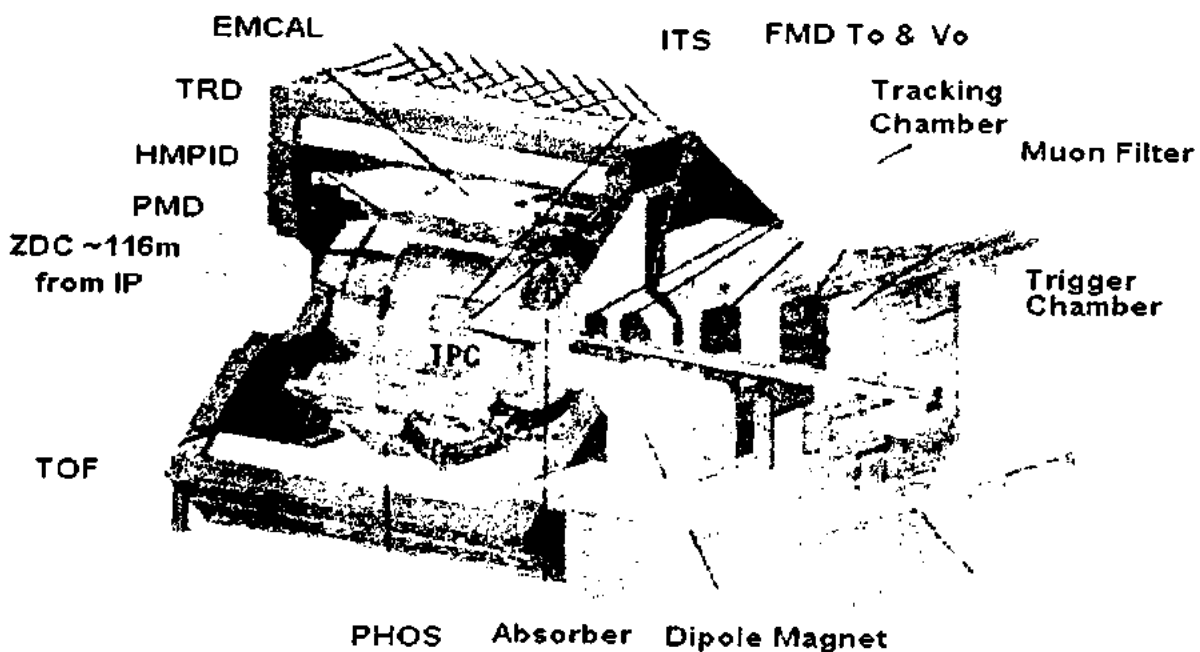
Figure 3.4   A Schematic Representation of ALICE. All Sub-Detector are also Indicated.
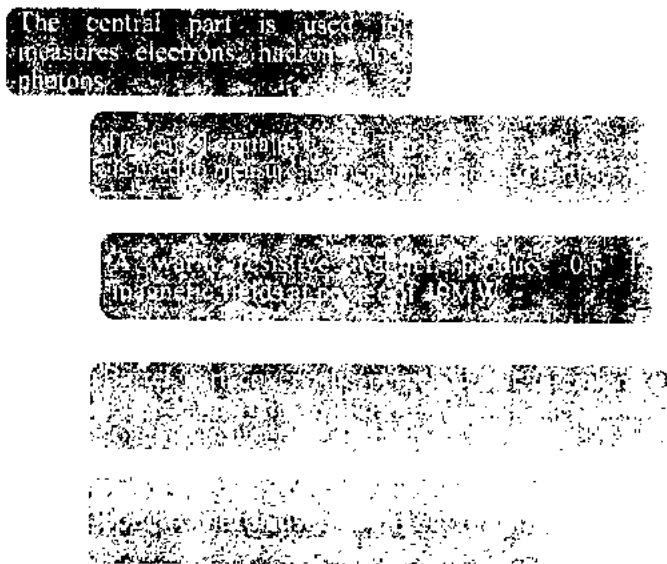
Figure 3.5 working of different parts of ALICE.

3.3.1.1 TRACKING DETECTORS

There are 6 layers of this silicon detector, it is called the Inner Tracking Detector (ITS). It is located at the midpoint of the ALICE detector. It indicates the contact point of the two conflicting beams of particle and also the decay of unstable particles. Spectrum of transverse momentum for particles is also seen by this. Externally the ITS have two highly committed Silicon Pixel Detector (SPD) and Silicon Drift Detector (SDD). 'x' and 'y' co-ordinate for each particle are recorded by these detectors.
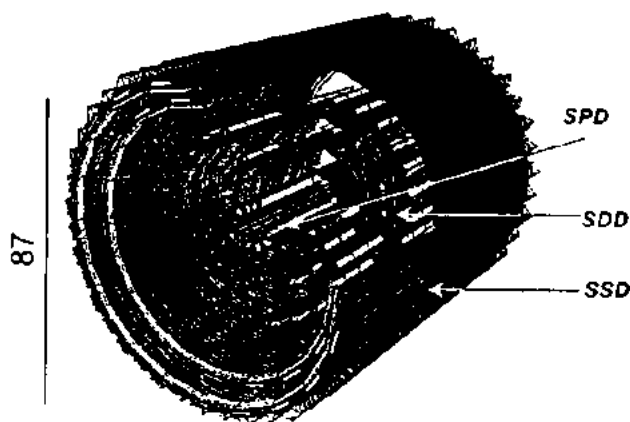
Figure 3.6 The Silicon Tracking System.

3.3.1.2 THE SILICON STRIP DETECTOR (SSD)

A pair of electron and hole is produced when a charged particle is permitted to passover a silicon wafer. The number of production of electron-hole pair depends on the energy loss of the particle and there is a current relation between them. Electron and hole start moving in opposite direction of the wafer when an electric field is provide. A strip of n-type is slot in to assemble electron and a strip of p-type to assemble holes. Both of the strips gathers equivalent amount of charges [44]. The whole configuration is shown in **Figure 3.7.**
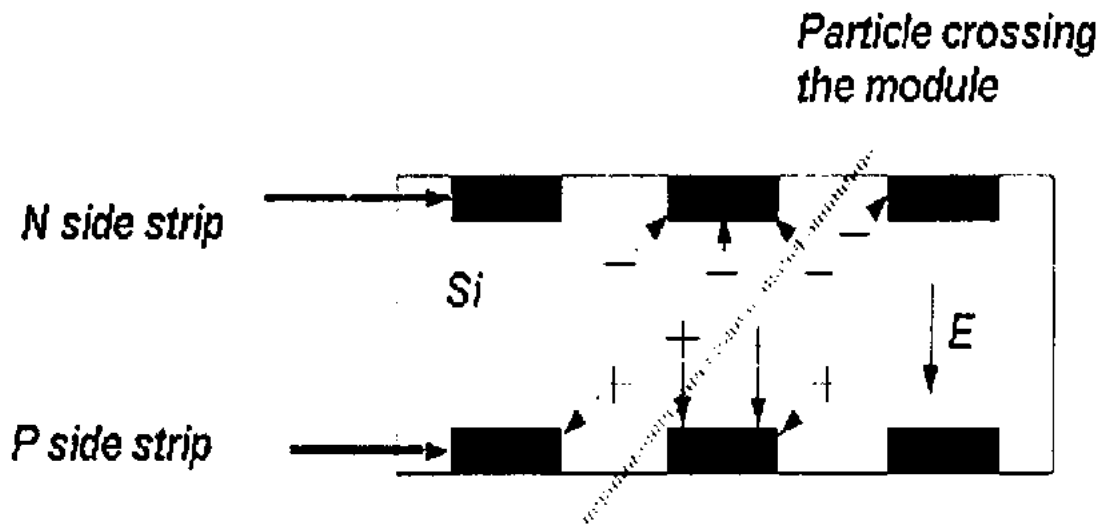
Figure 3.7 Silicon Strip Detector operations Principle.

3.3.1.3 SILICON DRIFT DETECTORS (SDD)

Its working is like the working of a gaseous drift detector. When a charged particle passes over this detector the electrons turned into free electrons and moves towards the P-type semi- conductor and then these free electrons make trajectories. The inferior side of this detector is a conductor it is very profound to heat. To chill the Silicon Strip Detector and Silicon Pixel Detector hard cooling systems and heat shields have been used inside [49]. The two layers of surface of the inner tracking system are silicon drifts detector. Their working scheme is akin to the working scheme of silicon drift detector but there is difference between them that these silicon drifts detector have P-type semiconductor at the upper side and n-type at the lowermost side of the detector. Holes and electron become free, when charged particles pass over them. These holes and electrons are then enticed

towards the semiconductor and to calculate the position of the particle the p-type and n-type semi-conductors are positioned at a small angle to each other [50].

3.3.1.4 TIME OF FLIGHT (TOF) DETECTOR

This detector is made up of Multi-Gap Resistive Plate Chambers it works at atmospheric pressure with the same efficiency. This Detector identifies particle and have high time resolution. TOF provide information about identification of particles by taking time difference between collision time and time when particle reach the TOF [45-46].

3.3.1.5 TIME PROJECTION CHAMBER (TPC)

In heavy ion collision such that Pb-Pb collision, a very large number of daughter particles can be fashioned but only because of large TPC. Up to 20.000 charged particle tracks can be handled by ALICE and it can also measure the momentum of the particle [47].

3.3.1.6 THE ELECTROMAGNETIC CALORIMETER

The EMCAL (Electromagnetic Calorimeter) is a detector which is designed to focus the measurement of photons from hard jets. It helps to increase jet energy resolution and aptitude of ALICE to measure more particles like electrons, neutral hadrons and high momentum photons [48].

3.3.1.7 THE PHOS DETECTOR

This detector consist of 17. 920 detection channels, it is a detector of very high resolution EM calorimeter. It is made of lead tungstate crystal which contains five modules, these modules are identical to each other and placed in a magnetic field.

The Range of pseudo-Rapidity is $-0.12 < \eta < 0.12$. PWO. It is inorganic and very fast scintillating crystal. The radiation n length of this detector is very short i.e. 0.9cm, which gives extraordinary benefits for calorimetry to use in high particle solidities. [51].

3.3.1.7 MUON SPECTROMETER

This detector detects and measure muons in the rapidity range of $-4 < \eta < -2.5$. The muon spectrometer has a large acceptanceat low transverse momentum i.e. ($2^{\circ} \leq \eta \leq 9^{\circ}$). At high transverse momentum the main production channel of J/ψ is through β-decay. This detector comprises: (i) a front absorber (ii) 5 muon tracking stations (iii) 1 dipole magnet (iv) 4 Resistive Plate Chamber Detectors (RPC) which separates into two stations. Momentum and energy of the fast moving muon can be calculated when it pass through the solenoid magnet. The absorber removes the low momentum muons so that only high momentum muons from J/ψ may left alone for high momentum muon detection [52].

3.4 ALICE OFFLINE FRAMEWORK

Huge data is created in heavy ion collisions and it was a big challenge for the physicists to handle such a large amount of data. Therefore, to get particular and precise simulation results of data produced by ALICE detector, physicists have developed unique algorithms which are used for the analysis of data. The combination of these algorithms is commonly known as ALICE offline framework. Different particles transport packages have been produced through virtual machine by using Monte-Carlo technique which allows control at run time between packages. The ROOT framework was adopted after an intense evaluation period in November 1998 and immediately the improvement of the ALICE offline Framework was started [53-54]. ROOT framework is an important part of the Offline framework which is used to handle at applications at large scale.

ALICE users have now a framework which is exclusively in C++. With the help of AliRoot software all the scientific design information have been parroted and license developers to deal with two things first the instant requirements and secondly the lasting objectives in the same framework with the help of contribution to all users of ALICE.
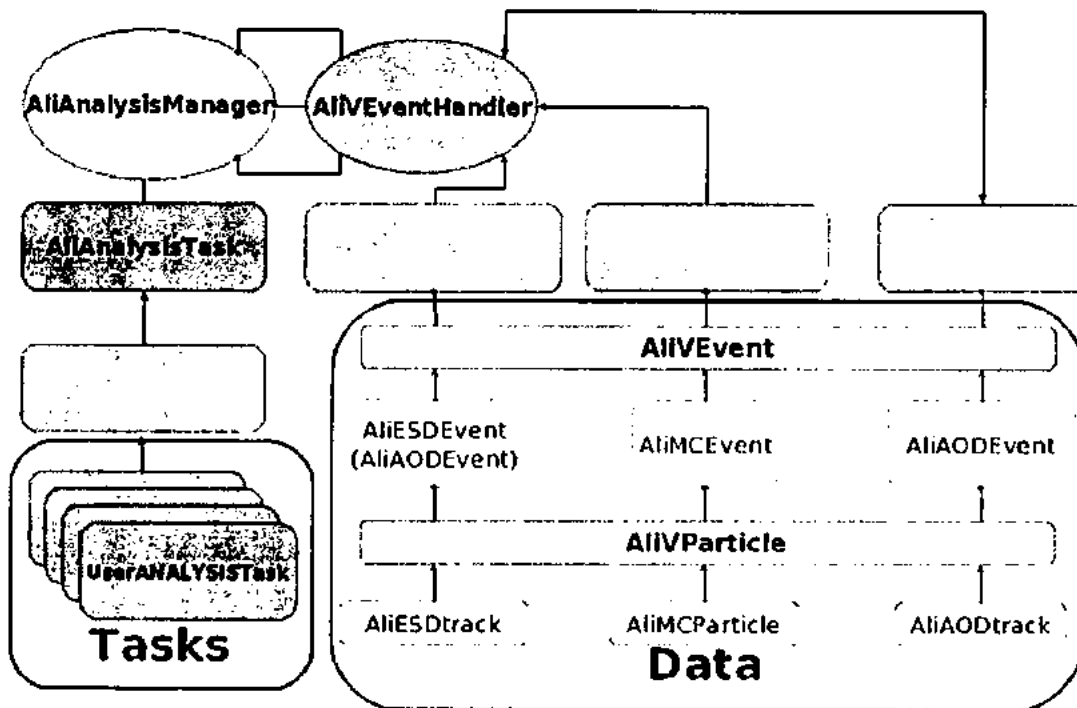

Figure 3.8 The Overall Picture of ALICE Offline Framework.

26

3.5 MONTE CARLO SIMULATION

John von Neumann, Nicholas Metropolis and Stanislaw Ulam invented the method of Monte Carlo Simulation in 1940, while working on the project of nuclear weapon designing and after that it was named as Monte Carlo Casino [55].

The name comes from the similarity of the technique to the act of playing in a real gambling casino and also keeping and recording the results. Monte Carlo methods are a comprehensive class of computational algorithms that depend on repeated random sampling in order to obtain numerical results. Typically one runs simulations many times over to gain the distribution of an unknown probabilistic article. Physical and mathematical systems can be simulated with the help of Monte Carlo methods. It is more suitable to derive a scientific result by a computer using these methods If it is difficult to deduce it with a deterministic algorithm [56].

While using the Monte Carlo Methods, the systems involve many degrees of freedom, like fluids, strongly coupled solids, disordered materials and cellular structures can easily be simulated. These are widely used in mathematics and physics to evaluate complex problems that cannot be solved by using deterministic algorithms. When Monte Carlo methods are being applied in the exploration of space and oil, their forecast of failures are routinely better than other alternative methods [57]. Monte Carlo Methods have a lot of applications in engineering, electronics and geo-statistics etc. Giving different levels of uncertainty, energy outcome of wind farm during its lifetime can also be simulated. Effects of pollution by diesel and petrol can also be simulated with the help of Monte Carlo Methods [58-59]. Numerical optimization approach is a dominant and well-known purpose of arbitrary numbers in numerical simulation. In this context, it is used to minimize or maximize some vector functions having large number of dimensions.

3.6 THE ROOT SOFTWARE

Root is an object oriented program, developed in CERN in 1994 by Rene Brun and Fons Rade Makers. It contains C and C++ interpreter and compiler and is particularly used for, reading and writing data files, plotting, and for data analysis. Due to these properties it exquisitely fits in high energy physics. It can stock large files and extensively based on C++ language. ROOT can provide the following packages.

Analyses functions and distribution, diagrams and histograms, Matrix Algebra, four vectors computation, three dimensional visualizations. it can analyses multi variety's data

by unseeing neural network and by means of Grid, access to distributed data can be obtain moreover interfacing Python and Ruby can be obtained in both directions.

Tree is the main article of ROOT software which is a data ample. Just like a natural tree it is consist of branches and leaves (substructures). The Tree has a large storage aptitude and sliding window to underdone data. It has been used for high computing efficiency. The data from LHC experiment are handled by ROOT. Mostly plots and results of presently experiment are acquired by this software.
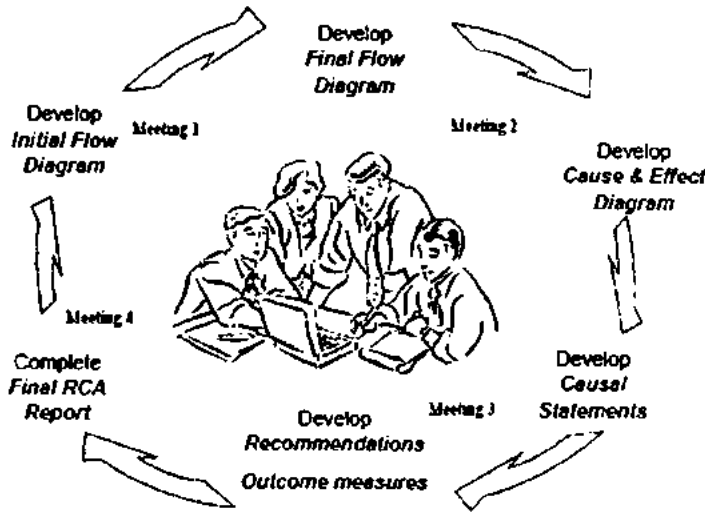

Figure 3.9   The overall pictorial concept of Root Analysis.

3.7   ALIROOT

At different stages of the simulation process AliRoot structure can offer data, in this way it can offer the nearly stable simulation of detector response and progress of the detector design.

The central module in AliRoot framework is called STEER. It offers routing, base classes, interface classes and run management. Every detector has independent modules which include simulation code, reconstruction and the analysis code. A whiteboard approach is developed where the shared data is placed to ROOT memory which is then available to all modules. With the help of tasks for interactive browsing, common and repeated methods could be raised. In AliRoot, reconstruction and analysis procedures are done by tasks.

An abstract interface called AliGenerator is developed to make possible the use of different generators. Study of full events, event by event analysis, single processes or in both of the cases, can be done with this interface. By applying this theoretical foundation

class, numerous codes of Monte Carlo simulations such as PYTHIA, HERWIG and HIJING are available from the classes of AliRoot [60-61]. Another interface is developed with FLUKA, using Virtual Monte-Carlo to provide another substitute to GEANT3.

3.8 FLUKA (FLUktuierende KAskade) A PARTICLE TRANSPORT CODE
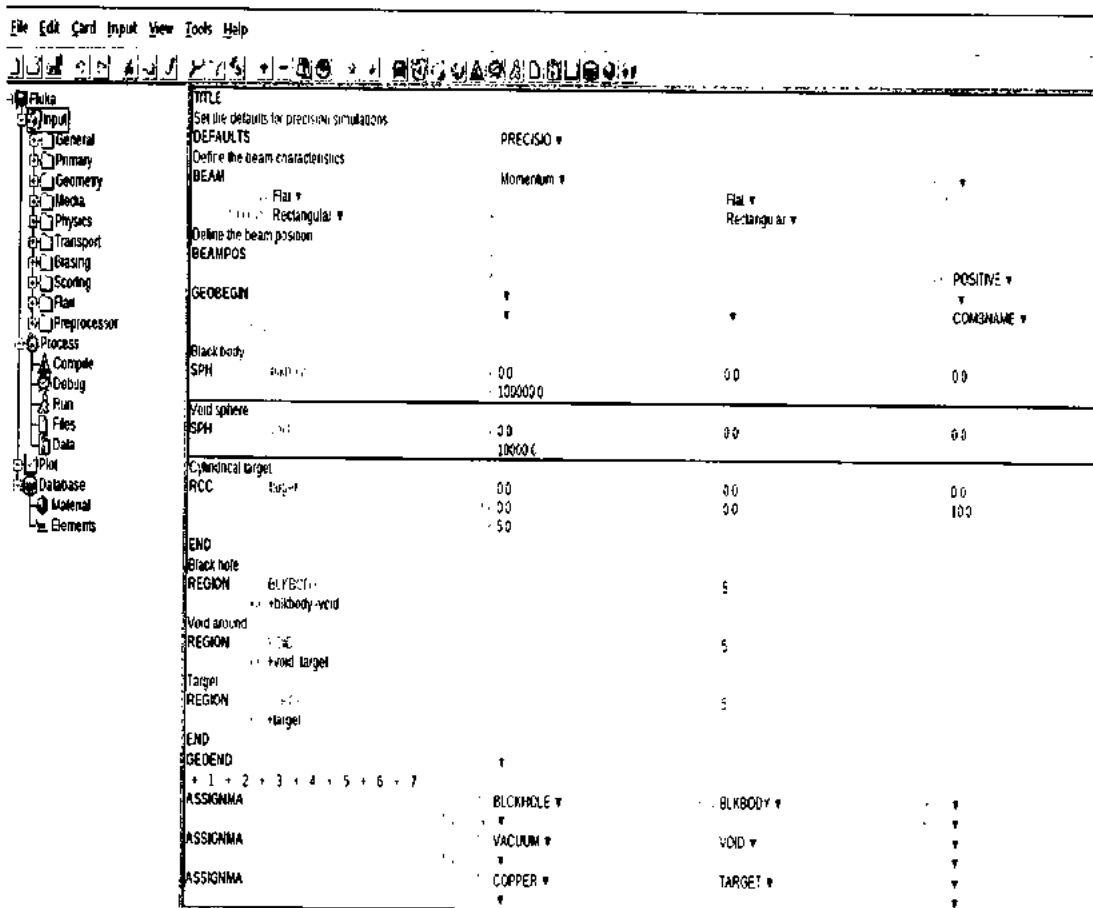
Figure 3.10   Schematic print out of general FLUKA input file

FLUKA is a broad functional tool for the reckoning of particle transportation which covers a comprehensive range of applications. It is a wide-ranging tool for the scheming of particle transport and interfaces with matter. It covers an protracted range of applications i.e. proton and electron accelerator shielding, target design, dosimetry and radiation protection, neutronics, calorimetry, tracking and detector simulation, detector design, accelerator driven Systems for example Energy Amplifier, cosmic ray research, space radiation (space related studies partially funded by NASA), neutrino physics, hadron

therapy and beam dump etc. It is a fully integrated Monte Carlo Simulation package for the interface of particles and nuclei in matter [62-64]. Few dominant properties of FLUKA are:

- Uniformity is safeguarded among all the reaction steps and reaction types.

- Predictivity about possibly produced particles is provided when experimental data is not directly available.

- Conservation laws are imposed at each step.

- Results are checked against experimental data at single interaction level.

Moreover, we can simulate the transportation of nearly 60 different particles in matter

- Proton-proton and proton-nucleus interactions up to 10000 TeV.

- Heavy ion interactions up to 10000 TeV/n.

- Electromagnetic and μ interactions from 1 keV to 10000 TeV.

- Energy loss and transport of charged particle.

- Transport in magnetic fields.

- Transport and interactions of multi-group neutron sup to 20 MeV.

- Neutrino interactions up to 100 TeV.

We can also transport Synchrotron radiation and optical photons using this program. Tracking of emitted radiation from unstable lingering nuclei and time evolution can be achieved online. Improvement of sound and modern physical models is the highest priority of design and development of FLUKA. While developing FLUKA, microscopic models are used on every possible occasion, reliability among all the reaction types is ensured and the results are verified with the experimental data [65]. Methodical use of double accuracy had a vast impact on overall precision which makes this code very efficient. These qualities are achieved by making cautious choice of the algorithms used. A sensible elasticity is attained by lessening the need for user-written code and provides a large number of choices to the user.

FLUKA package has dual capability. It can be utilized in fully analogue mode and also in biased mode in contrast with any other software. It has been used for the forecast of fluctuations, signal chances and other associated events, an enormous variety of

arithmetical techniques are also accessible to examine other occasional events in association with mitigations by several preparations of magnitude. The performance and development of sound and contemporary physical models is an extraordinary characteristic of FLUKA. It can hold even very difficult geometries, using an enhanced version of the well-known Combinatorial Geometry (CG) package. The FLUKA Combinatorial Geometry has been considered to observe correctly charged particles tracks even in the presence of magnetic or electric fields. FLUKA geometry is the part of the code where effectiveness, precision, reliability and flexibility have joint altogether and offering very valuable results. It is consequential of the Combinatorial Geometry package and it has been completely revised. A completely new, quick pursuing approach has been established with distinct consideration to charged particle transport, particularly in magnetic fields. New figures have been launched ensuing improved rounding precision, speed and with easier input preparation. A variety of visualization and debugging tools are also obtainable. In many purposes no programming is obligatory from the user. Yet, a number of user interface practices are offered for users with particular necessities.

Through recurrent remedy to table look-up sampling, and by efficient use of dual exactness the overall accurateness and proficiency can be attained. These potentials have profited from a cautious selection of the algorithms adopted. To manage a logical elasticity while curtailing the essentials for code written by user, this package has been delivered with a variety of choices accessible to the user. FLUKA uses a unique transport algorithm for charged particles together with a multiple Coulomb scattering handling, bountiful for the accurate imaginative shift even near a boundary. A unique handling of multiple Coulomb scattering and of ionization fluxes allows the code to manage precisely some complicated tasks, such as electron backscattering and energy deposition in thin layers even in the few keV energy range.

An advance and user friendly interface of FLUKA is known as flair. This interface makes easy edit of the input file, run codes and observe the output. It is based exclusively on Python. Flair offers following functionalities:

➢ An almost error free and easy editing interface known as front-end interface which is used for correction of errors of the user input during editing.

➢ During a run it provides compiling, debugging and scrutinizing of the status.

➢ Processing of output files and generation of plots is done by an interface known as 'gnu plot' which is a back-end interface.

> It geometrical objects for easier editing, accumulating and sharing among projects of other users.

> Python is used for operating the input files, processing of the outcomes and for interfacing to 'gnu plot'.

Flair mechanism is direct with the FLUKA input file and is capable to read/write all suitable FLUKA input setups. The user is interacting instantly with the FLUKA cards inside the flair editor, having a small conversation with every card which displays the information in human understandable format. Flair is capable to read and write all layouts recognized by FLUKA, therefor internally it works always in the names format and tackles the input as a list of comprehensive cards. The built-in format for saving is constantly fixed with names for the input and free with names for the geometry. The user can dominate the default exporting format either by the appropriate FLUKA cards (like **FREE, GLOBAL, GEOBEGIN**) or by overriding the format in the project definition. Future expansions of FLUKA comprises intensification of the physics models for new ions, such as oxygen and helium, with an interpretation to their possible use in hadron.

CHAPTER 4

RESULTS AND DISCUSSIONS

The simulated results regarding production of pions in Pb-Pb interactions at various collision energies are presented in this chapter. These results are obtained by using Monte Carlo Simulation technique i.e. with FLUKA software. The energy distribution and spectral flounce of produced secondary particles during the collision are observed by these Monte Carlo Simulation packages. The data collected is then compared, analyzed and demonstrated in a broad way. The illustration of data analysis is important because in just few graphs it could not be explained. Some other related factors for example heavy ion interaction models constructional geometry of detector in brief is also included in this chapter.

4.1   Heavy Ion Interaction Models

There are many models for heavy ion interactions. The energy range of these models differs from each other.

1. **for E > 5 GeV/n** (Dual Parton Model (DPM))

   DPMJET-III: This model has used in the study of my research work and related simulations, in its third version. **DPMJET-III** is even used for the photo production off nuclei and the size of the code is about 90,000 lines. It is Monte carlo event-generator for the simulation of high energy hadronic interactions for example hadron-hadron collations, hadron-nucleus collisions, nucleus-nucleus collisions. Its energy ranges from 5 GeV/nucleon to 10^{11} GeV/nucleon. FORTRAN77 is used as its programming language.

DMPJET's interface to FLUKA can be understood by the following example:

FLUKA → REQUEST: single nucleus- nucleus interaction (A+A)

DMPJET → A+A → p, n, π^+, π^-, ...excited fragments

FLUKA → Evaporation, fragmentation, de-excitation of fragments and transport of produced hadrons.

2. **for 0.1 GeV/n < E < 5 GeV/n** (Relativistic Quantum Molecular Dynamics Model (Relativistic Quantum Molecular Dynamics) RQMD-2.4)

3. **E < 0.1 GeV/n** (Boltzmann Master Equation (BME) theory, BME)

In electromagnetic dissociation we use FLUKA ae well as for the evaporation Fermi breakup fission and γ-de-excitation. Collectively we say that FLUKA can handle all types of particle transport [67].

4.2 SIMULATION PARAMETERS AND GEOMETRY

Two coaxial cylinder are used in this simulations. The cylinder at which the Pb-Pb beams collisions took place has z-axis as its axis of collision. Two (RPP) right parallelepiped cylinders are used as a vacuum and black body. We have also created a geometry of a sphere which acts as an interaction point (I.P) named SPH I.P. Five primaries have used in simulation, number of events are 10,000 and lab momentum is energy into atomic mass of lead. i.e. 207 × 1 TeV (10,000 GeV).

```
RPP  blakhole     -5000000.  +5000000.  -5000000.  +5000000.  -5000000.
+5000000.
RPP  vacumbox     -10.0 +10.0 -10.0 +10.0 -10.0 +10.0
SPH  I.P.         0.  0.  0.  0.01
```

4.3 PIONS PRODUCTION IN Pb-Pb COLLISIONS AT VARIOUS ENERGIES USING FLUKA SOFTWARE

In Pb-Pb collisions, the behaviour of energy spectrum of pions production can precisely and accurately be measured at LHC energy range. The observed patterns of energy spectrum of pions in Pb-Pb collisions at different energies by using FLUKA package are presented and discussed here in this section. In FLUKA, Monte Carlo simulation technique is used for the recording of results which is called scoring. FLUKA can activate several pre-defined estimators and users can even build their own scoring by user routines, THOUGH Built-in scoring covers most of the common requirements. It's been widely tested and takes consider BIASING weights automatically. It has effective programs to evaluate statistical errors and refined algorithms for track subdivision.

Scoring can be geometry dependent AND/OR geometry independent. Particle fluencies, current, track length, energy spectra, Z spectra, energy deposition can be scored by FLUKA.

Few scoring commands by FLUKA are as follows:

USRTRACK, USRCOLL: $d\varphi/dE$ (differential fluence) of a given type or family of particles can be scored in a given region.

USRBDX: Scores average $d^2\varphi/dEd\Omega$ (double-differential fluence or current) of a given type of particles on a given surface.

USRBIN: Spatial distribution of energy deposited, total fluence in a regular mesh (cylindrical or Cartesian) which is described by the user can be scored in its average value by using this command.

USRYIELD: Dispersal with respect to energy and angle and even for the other more "exotic" quantities double differential yield of particles evading from a surface can be scored by using this command.

SCORE: This command scores energy deposited in all regions. [68].

We have simulated the four energy level of lead particles that is 0.5 Tev, 1 Tev, 1.5 Tev, and 2 Tev. The fluence, double differential fluence and angular distribution has been studied and discussed at different energies.
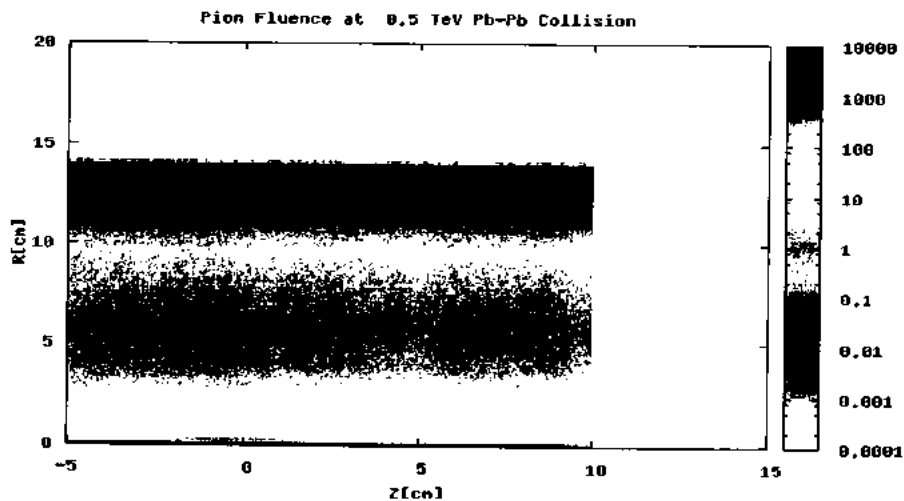
4.4 RESULTS OF PIONS FLUENCE ESTIMATION

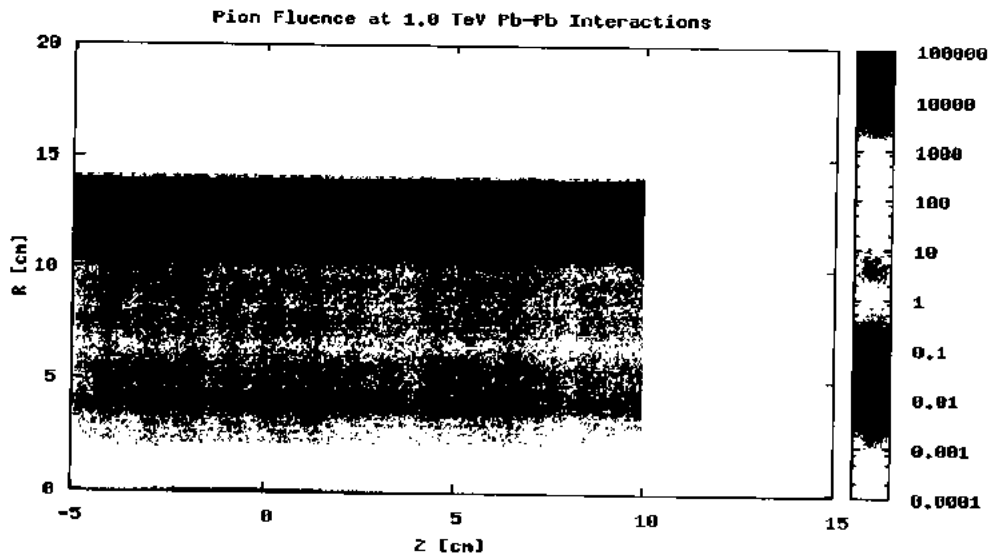**Figure 4.1** Two dimensional view of Pions (π^+, π^-, π^0) fluence at 0.5 TeV.

Pion Fluence at 1.0 TeV Pb-Pb Interactions

Figure 4.2 Two dimensional view of Pions (π^+, π^-, π^0) fluence at 1.0 TeV.

Pions Fluence at 1.5 TeV
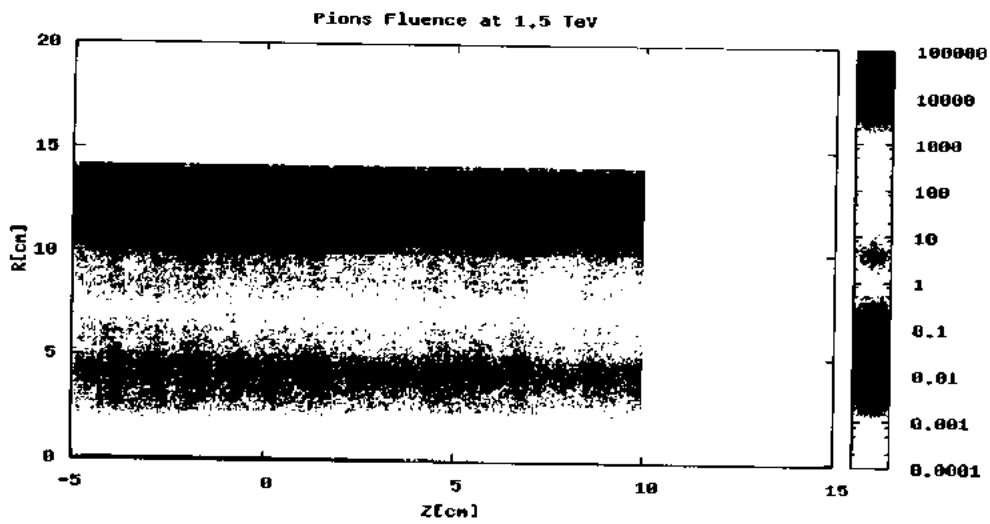
Figure 4.3 Two dimensional view of Pions (π^+, π^-, π^0) fluence at 1.5 TeV .

Pions Fluence at 2.0 TeV

Figure 4.4   Two dimensional view of Pions (π^+, π^-, π^0) fluence at 2.0 TeV.

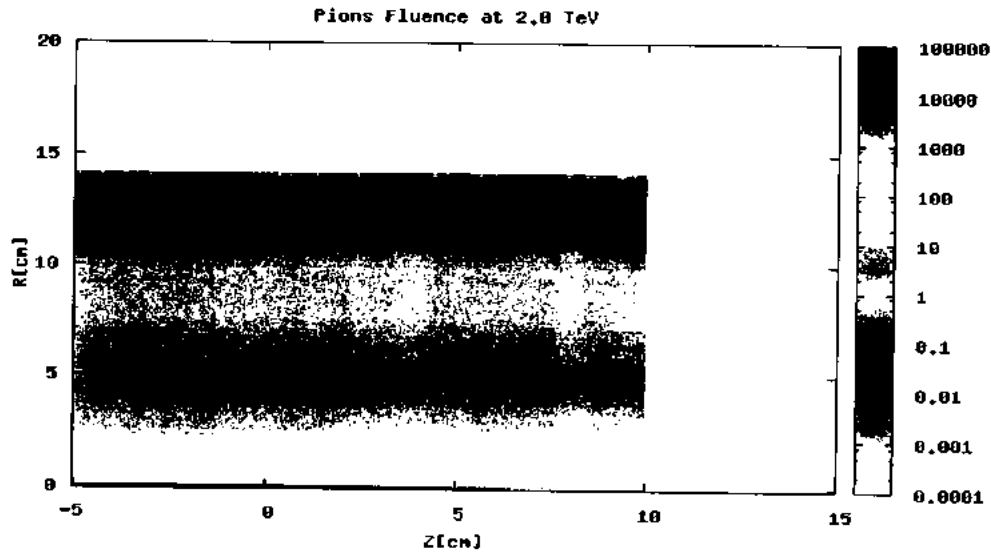In above graphs pions fluence is shown at energies 0.5 TeV, 1.0 TeV, 1.5 TeV and 2.0 TeV respectively. These graphs are presenting two dimensional view of pion production in Pb-Pb collision, which is taking place in a hollow cylindrical particle production region and cross section of this particle production region is presented here. The z axis of the cylinder (in which collision took place) is taken along horizontal axis (in cm) and radius of the cylinder (in cm) is taken along the vertical axis. The different color bands are showing the production of pions at different energies, the wider bands have high number of produced particles while the narrow bands have low particle production rate. The scale on the right side is showing the production scale of daughter particles at energies given at left for example the energy of yellow region is between (100 to 1000) GeV. If been observed keenly then the particle production is visible within these color bands. These graphs are giving a bulk picture of Pions production. The particle production increases as we increase the energy.

37

4.5 PIONS DOUBLE DIFFERENTIAL FLUENCE ESTIMATION AND RESULT DISCUSSIONS

As described earlier, the above graphs which were presentng two dimentional view of particle production were providing a bulk information of particle production, it is not possible to have a precise knowledge of type of the pion which is produced at the primary energies which are taken to be 0.5 TeV, 1.0 TeV, 1.5 TeV and 2.0 TeV. In the following graphs we are going to discuss the double differential fluence which means we are now taking into account the fluence of partice with respect to energy of particle and angle of deflection of particle. Moreover the following graphs are ploted to provide a precise information about the production of pion at individual level of each type of pion at each primary enegy. For example now I am going to discuss the double differential fluence across the interaction point for π^+, π^- and π^0 separately each at one of the prime energy that is 0.5 TeV here.
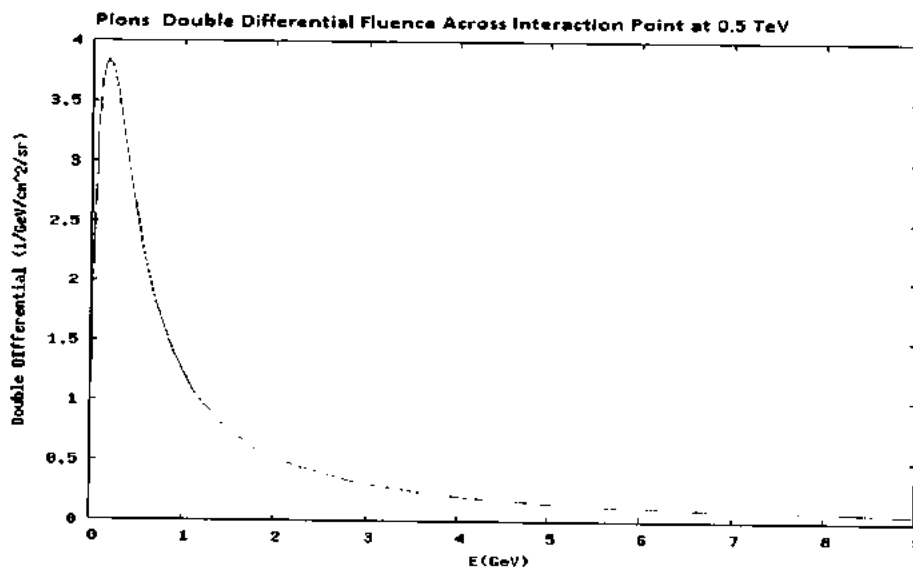
- **Pions production at 0.5 TeV.**
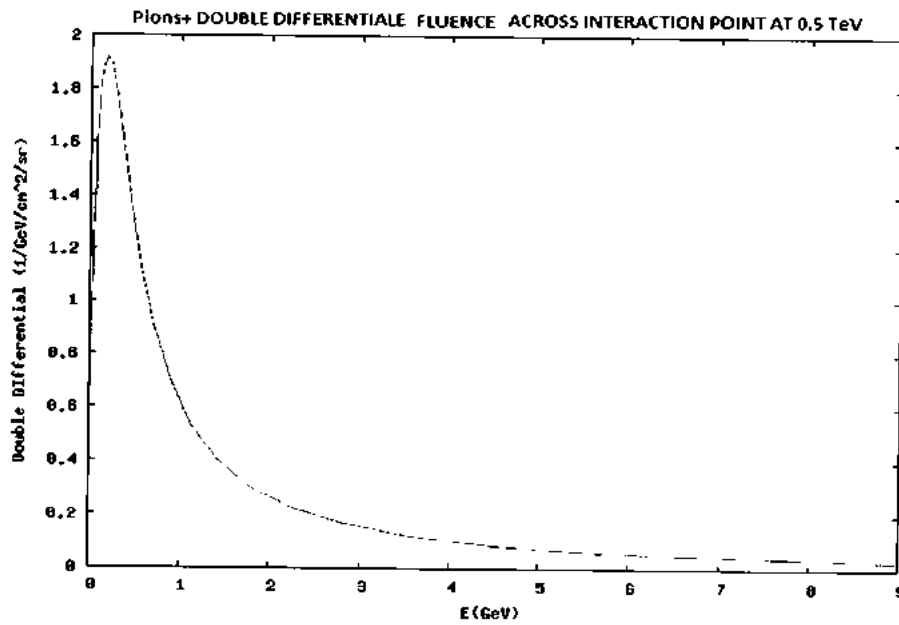

Figure 4.5   Double Differential Fluence of π^0 at 0.5 TeV.

Pions+ DOUBLE DIFFERENTIALE FLUENCE ACROSS INTERACTION POINT AT 0.5 TeV

Figure 4.6   Double Differential Fluence of π^+ at 0.5 TeV

PIONS -- DOUBLE DIFFERENTIAL FLUENCE ACROSS INTERACTION POINT AT 0.5 TeV
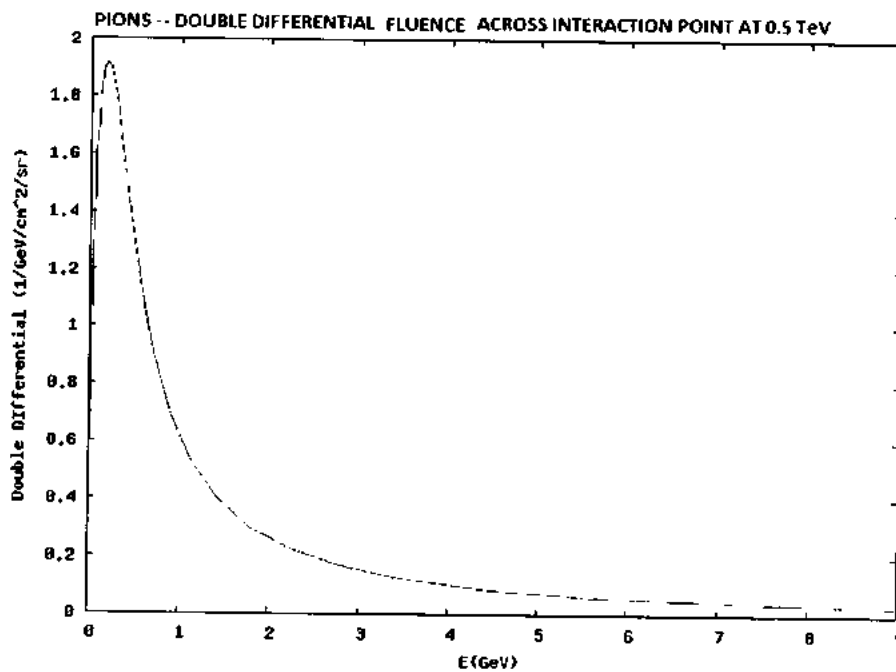
Figure 4.7   Double Differential Fluence of π^- at 0.5 TeV

In **Figures 4.5 to 4.7** double differential flounce of pions π^0, π^+ and π^- respectively is presented. We are taking energy of produced daughter particles along x-axis and double differential flounce count along y-axis. Looking at **figure 4.5** it is clear that peak which is depicting maximum number of π^0 are producing is between 0 to 0.4 along x-axis and it is

39

between 3.5 to 4 along y-axis and as the energy of secondary or daughter particle is increasing particle's double differential count decreases exponentially. The same culture can be indicated in **Figures 4.6 and 4.7** where the peak is between (0 to 0.4) along x –axis and (1.8 to 2) along y-axis. There is inverse relation between the energy of secondary particles and double differential count of the produced particle. These graphs are plotted by taking 0.5 Tev as primary energy.
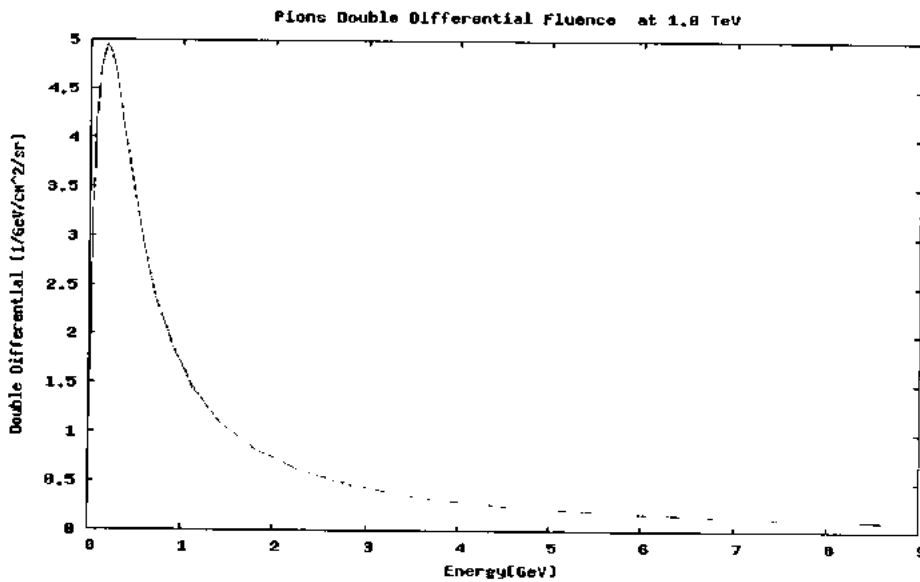
- **Pions production at 1.0 TeV.**

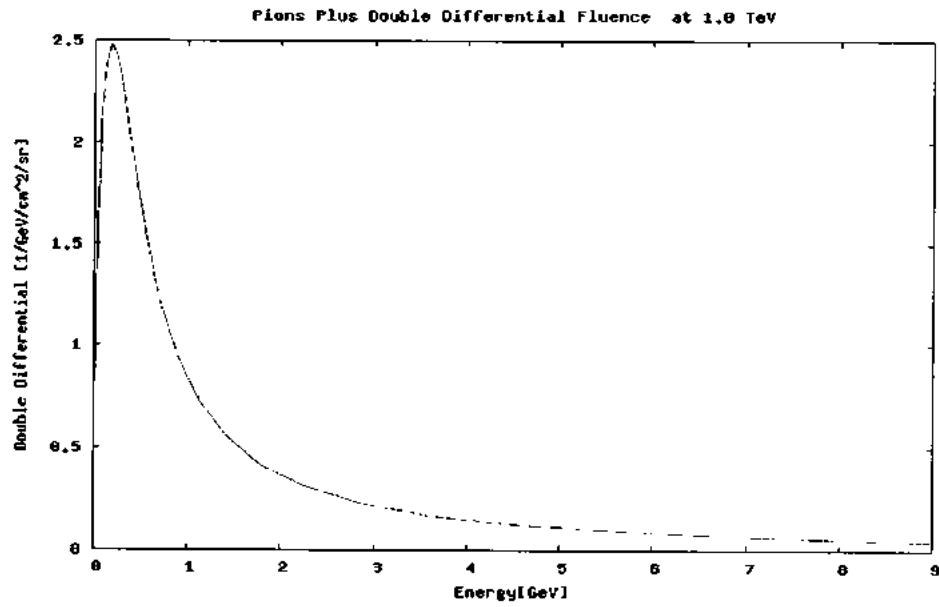**Figure 4.8**   Double Differential Fluence of π^0 across Interaction point of at 1.0 TeV

Figure 4.9   Double Differential Fluence of π^+ across Interaction point of at 1.0 TeV.
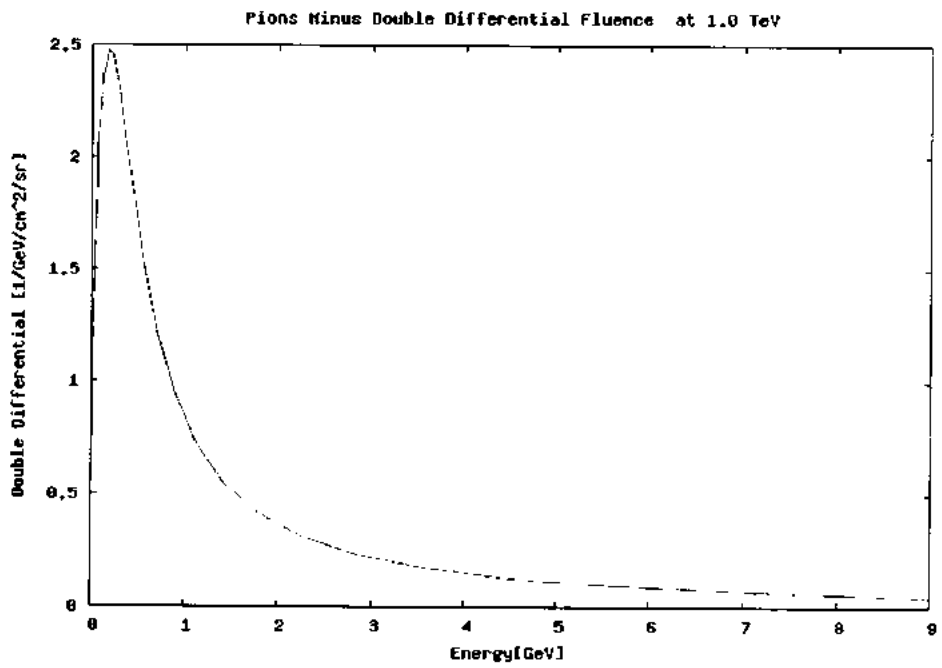
Figure 4.10   Double Differential Fluence of π^- across Interaction point of at 1.0 TeV.

In **Figures 4.8 to 4.10** double differential flounce of pions $\pi^0.\pi^+$ and π^- respectively is presented at primary energy 0.1 TeV. Energy of produced daughter particles in (GeV) is taken along x-axis and double differential flounce count (in 1/GeV/cm²/sr) is taken along y-axis. In **Figure 4.8** the peak is between (0 to 0.4) along horizontal axis and it is between (4.9 to 5) along vertical axis. On increasing the beam energy from 0.5 to 1 TeV the double differential count has also increased. Even in these graphs it is clear that as the energy of secondary or daughter particle is increasing along x-axis particle's double differential count is decreasing along y-axis. The same principles can be indicated in **Figure 4.9** and **Figure 4.10** where the peak is between (0 to 0.4) along x –axis and 2.5 along y-axis.it is evident from these graphs that there is inverse relation between the energy of produced secondary particles and double differential count of the produced particle. This inverse relation is due to the decay of pions as they started to exponentially decay into secondary products the double differential count of pions decreases rapidly.
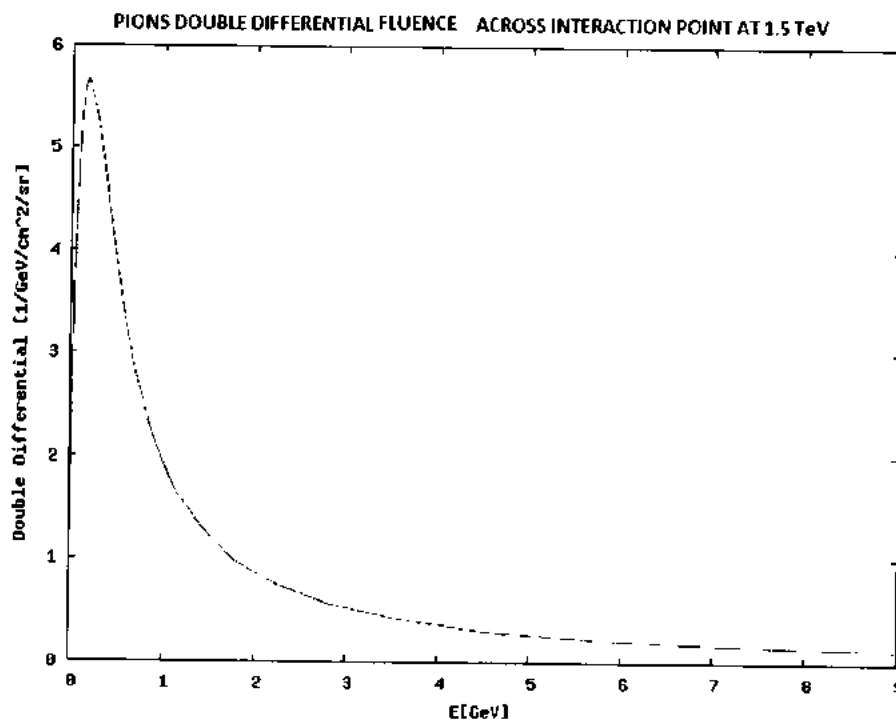
- **Pions production at 1.5 TeV.**

Figure 4.11   Double Differential Fluence of π^0 across Interaction point of at 1.5 TeV

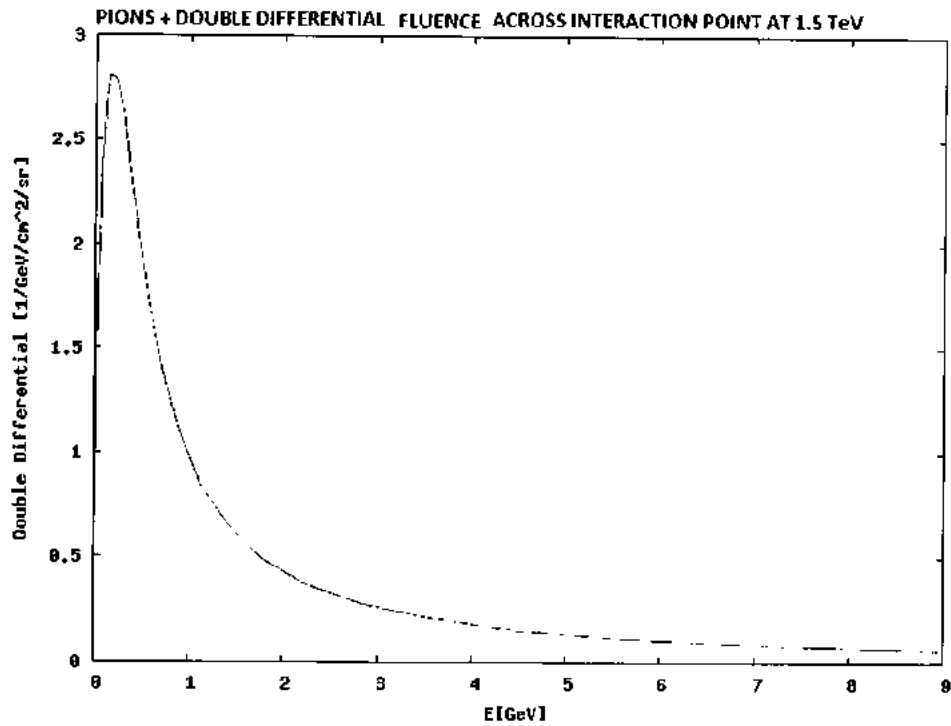PIONS + DOUBLE DIFFERENTIAL FLUENCE ACROSS INTERACTION POINT AT 1.5 TeV

Figure 4.12 Double Differential Fluence of π^+ across Interaction point of at 1.5 TeV.

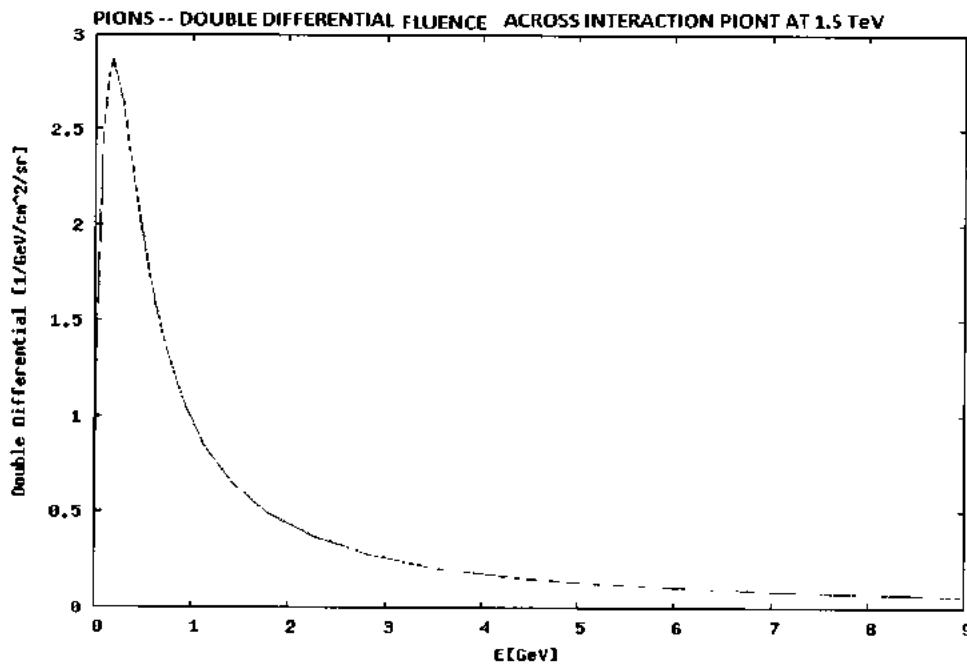PIONS -- DOUBLE DIFFERENTIAL FLUENCE ACROSS INTERACTION PIONT AT 1.5 TeV

Figure 3.13 Double Differential Fluence of π^- across Interaction point of at 1.5 TeV.

43

In **Figures 4.11 to 4.13** double differential fluence of pions π^0, π^+ and π^- respectively is presented at primary energy of 1.5 TeV. In **Figure 4.11** the peak is between (0 to 0.4) GeV along horizontal axis and it is between (5.5 to 6) $1/\text{GeV}/\text{cm}^2/\text{sr}$ along y-axis and as the energy of secondary or daughter particle is increasing particle's double differential count is decreasing. **Figure 4.12** and **Figure 4.13** are giving strength to this philosophy. In these peak is from (0 to 0.4) GeV along x –axis and (2.8 to 3) $1/\text{GeV}/\text{cm}^2/\text{sr}$ along y-axis.it is clear and obvious from these graphs that there is inverse relation between the energy of secondary particles and double differential count of the produced particle.

- **Pions production at 2.0 TeV.**
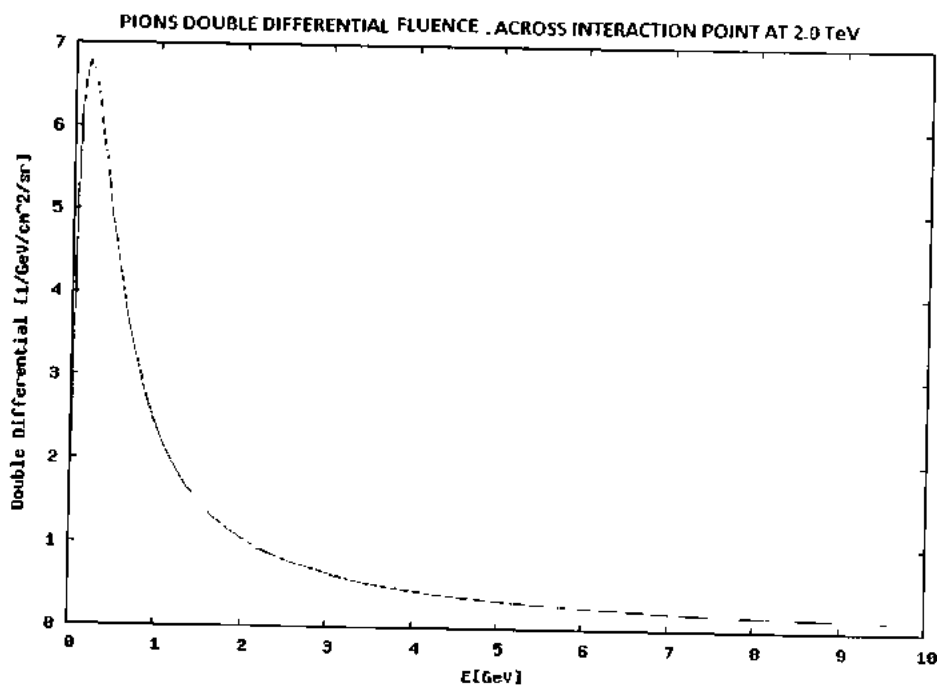

Figure 4.14 Double Differential Fluence of π^0 across Interaction point of at 2.0 TeV.
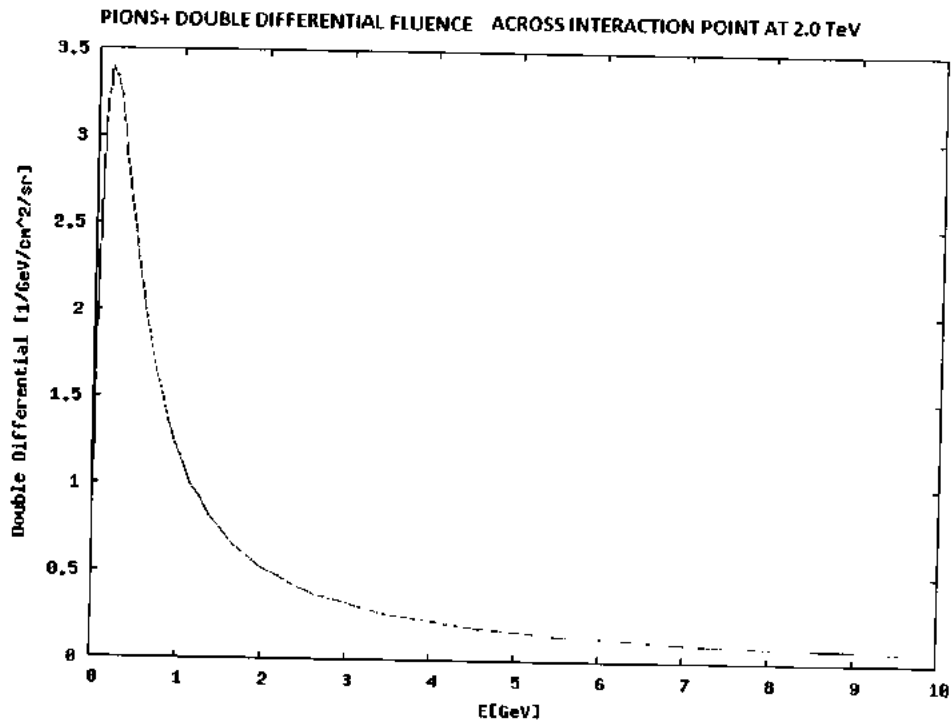
Figure 4.15   Double Differential Fluence of π^+ across Interaction point of at 2.0TeV.
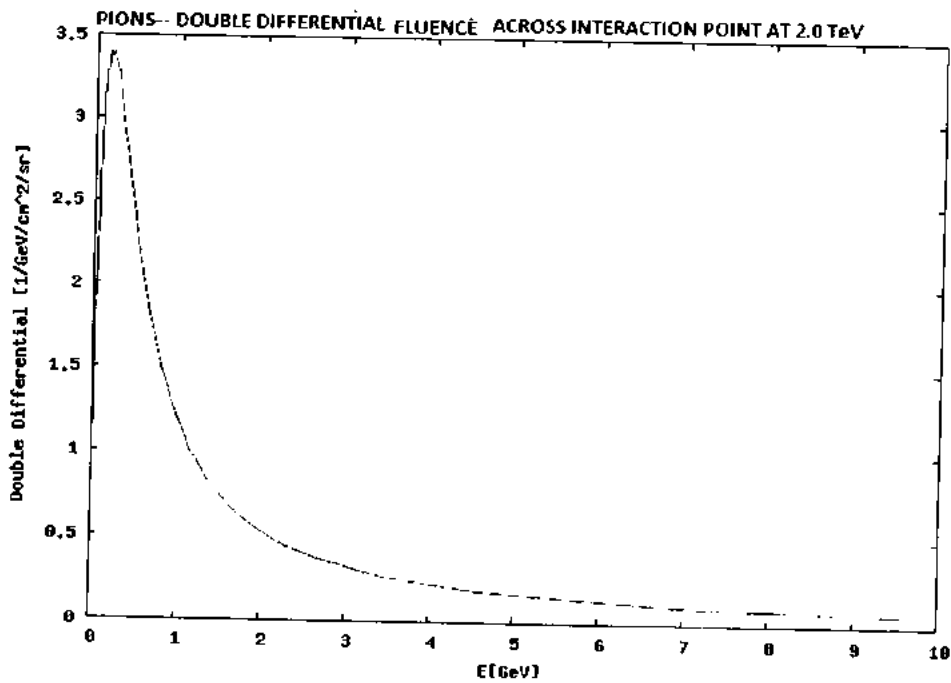

Figure 4.16   Double Differential Fluence of π^- across Interaction point of at 2.0TeV.

45

The above figures have been plotted by using Monte Carlo Simulation technique called FLUKA at different energy regimes. As a result of Pb-Pb collisions at very high energies, bulks of primary as well as secondary particles are produced. The objective of these graphs is to examine the production of pions ($\pi^\pm$ and π^o) which are secondary charged particles at different energy ranges. The energy spectrum of these charged particles is different at various energy levels. In this context, the energy spectrum of $\pi^\pm$ and π^o is made discretely which shows the consequences of FLUKA simulation of these charged particles at different energies. Figures show the flounce of pions at different energy regimes. The kinetic energy of the produced particles is taken along x-axis and the range of energy is 0 to 10 GeV while the double differential flounce is taken along y-axis.

In **Figures 4.14 to 4.16** double differential fluence of pions π^0, π^+ **and** π^- respectively is presented at primary energy of 2.0 TeV. These graphs are following the same fashion as in the earlier presented graphs, which are ploted at 0.5 TeV, 0.1 TeV and 1.5 TeV .The double differential count is maximum at 0.4 GeV along horizontal axis, it means that particles have attained their maximum lifetime here and after this point these particles started decaying into secondary particles and this phenomena has deceased the double differential count with the increasing energy of secondary particles. Through studying the above graphs we can conclude the same pattern that means: firstly an increasing pattern to sharp peak and then an exponentially decay along x-axis.

For a better comparison Now, the following graphs will provide a combine picture of particle production π^0, π^+ **and** π^- separately at all four primary energies taken into account. Which are 0.5TeV, 1.0TeV, 1.5TeV and 2.0TeV .

Figure 4.17: Fluence of π^0 at primary energies of 0.5 TeV, 1.0 TeV, 1.5 TeV and 2.0 TeV. A FLUKA's simulation snapshot.

Figure 4.17 is showing the fluence count of π^0 along y-axis while along x-axis energy of daughter particles is taken.it is clear from the figure that there is a drastic increase in the fluence count with the increase in beam energy. Along x-axis the π^0 particle has Its maximum lifetime at 0.4 after that the graph line started showing decay of π^0 and hence a decrease in flounce count with the increasing energy of secondary particle. This increase in particle fluence gets quite higher at 2 TeV.
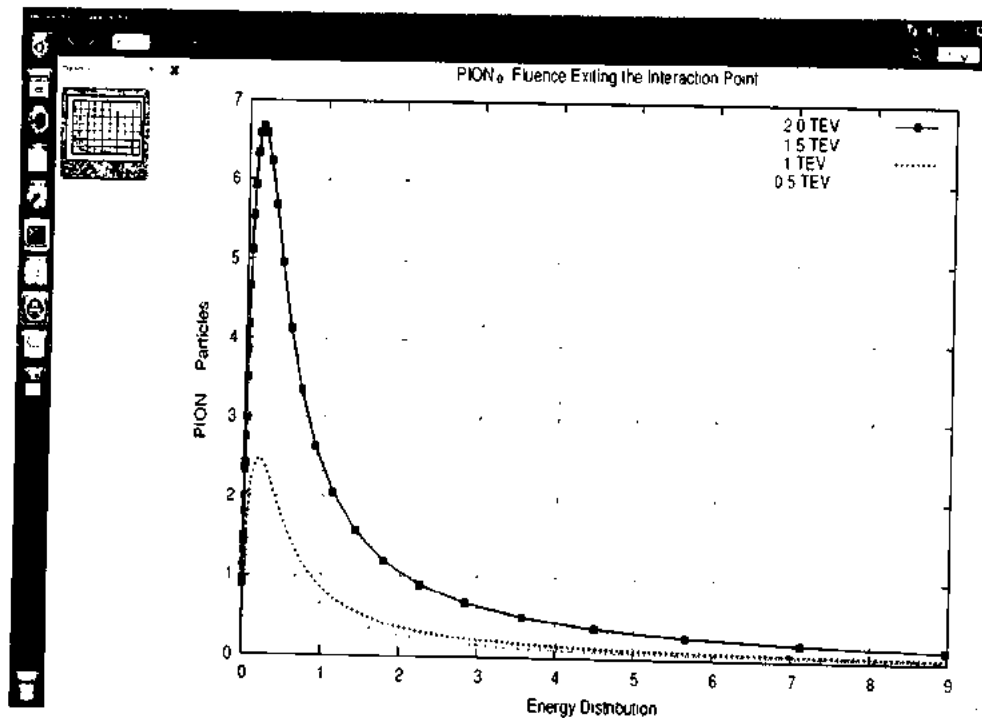
Figure 4.18 Fluence of π^+ at primary energies of 0.5 TeV, 1.0 TeV, 1.5 TeV and 2.0 TeV. A FLUKA's simulation snapshot.

Figure 4.18 is showing the increase in the fluence count of π^+ with the increase in beam energy. This increase is steady with the increase of beam energy and when the energy reaches to 2.0 TeV it reaches up to approximately 3.5. And if we look it along x-axis the π^+ particle has its maximum lifetime at 0.4 and ten there is an exponential decay of production of π^+. We can observe here an obvious decrease in flounce count with the increasing energy of secondary particle.
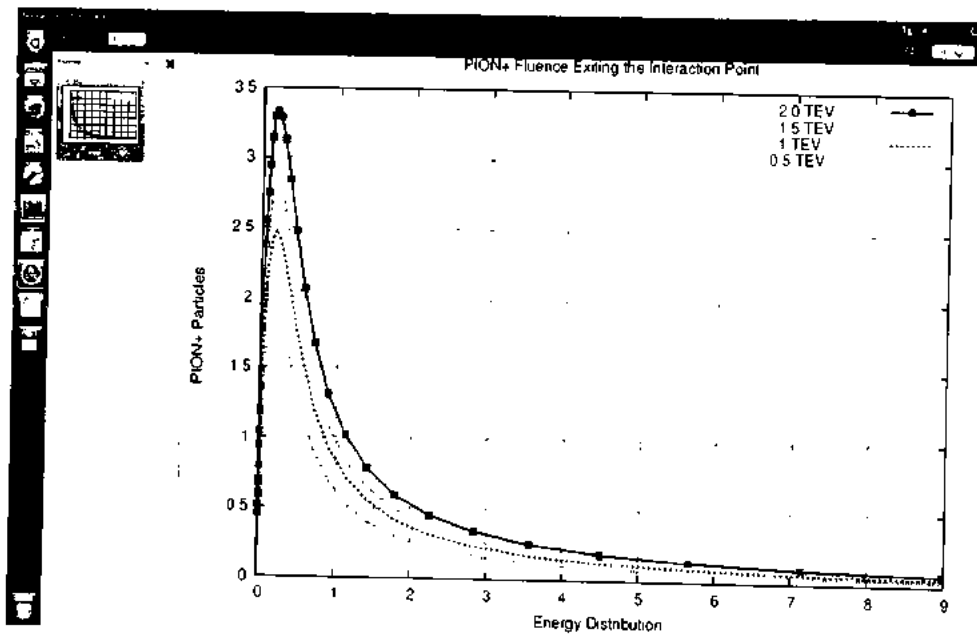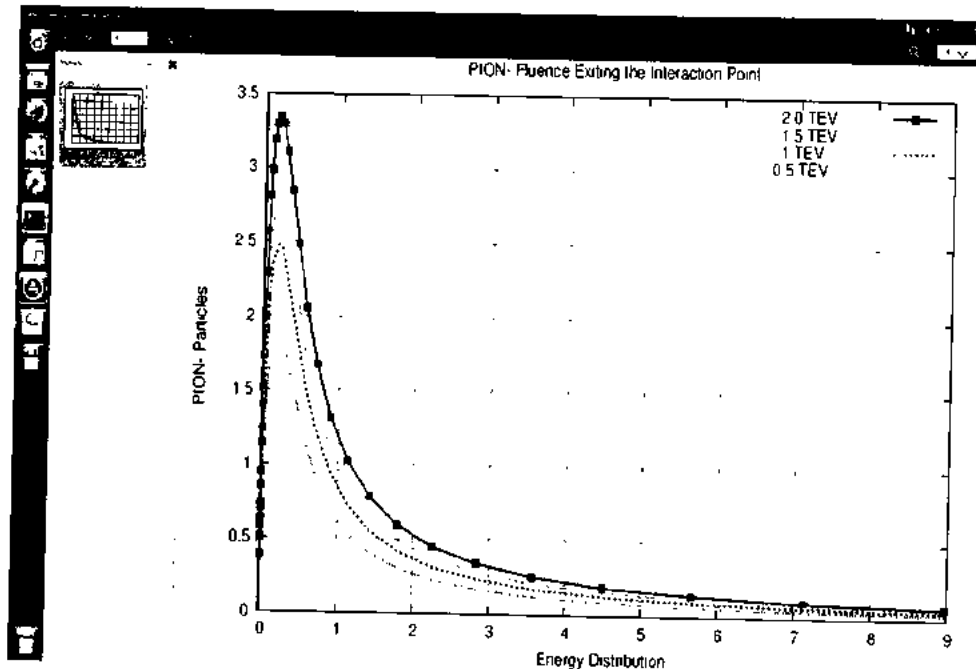
Figure 4.19 Fluence of π at primary energies of 0.5 TeV, 1.0 TeV, 1.5 TeV and 2.0 TeV. A FLUKA's simulation snapshot

Figure 4.19 is showing the increase in the fluence count of π with the increase in the primary energy and it is depicting the same fashion of **Figure 4.18** that is: attaining a sharp peak first and then to show a dramatic decrease continually, furthermore an increasing pattern of producing the π particle on increasing the primary energy.

4.6 ANGULAR DISTRIBUTION OF PARTICLES

While gone through the production picture of under discussion particles at 2D level, at individual level and then even at a combined pictorial level ,we have determined certain fashions of particle fluence . The concluding results are giving strength to each other by providing a same culture of production. Since this picture is still incomplete unless we include the angular distribution of produced particle that means we must take into account the angle of deflection of produced particle.

The angular distribution of the Pions is shown below at 0.5 TeV, 1.0 TeV, 1.5 TeV and 2.0 TeV respectively

Pions Angular Distribution Exiting Interaction Point at 0.5 TeV

Figure 4.20   Angular Distribution of Pions at 0.5 TeV.

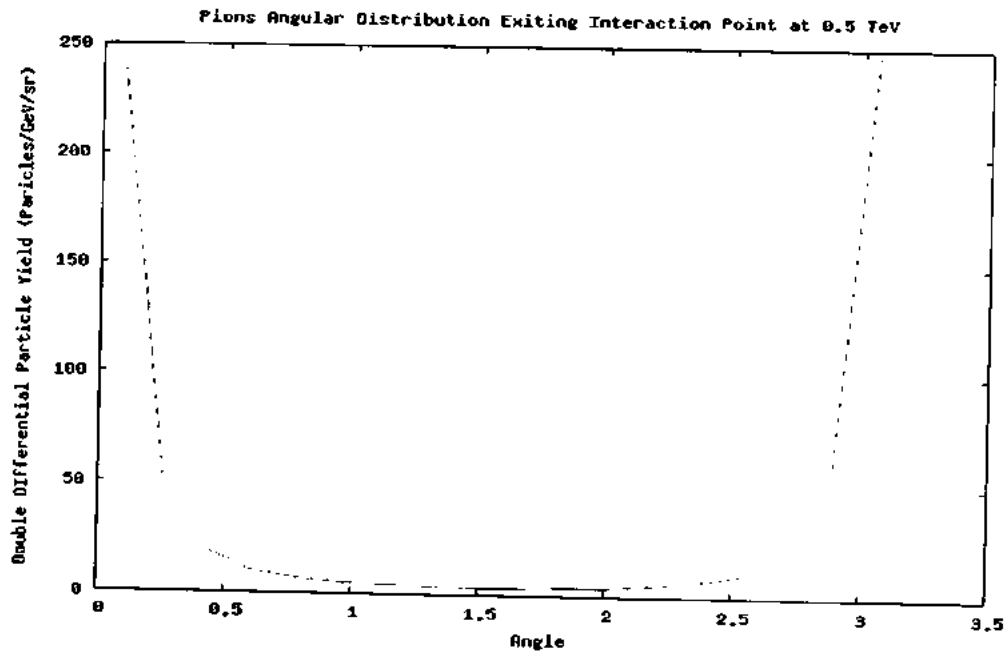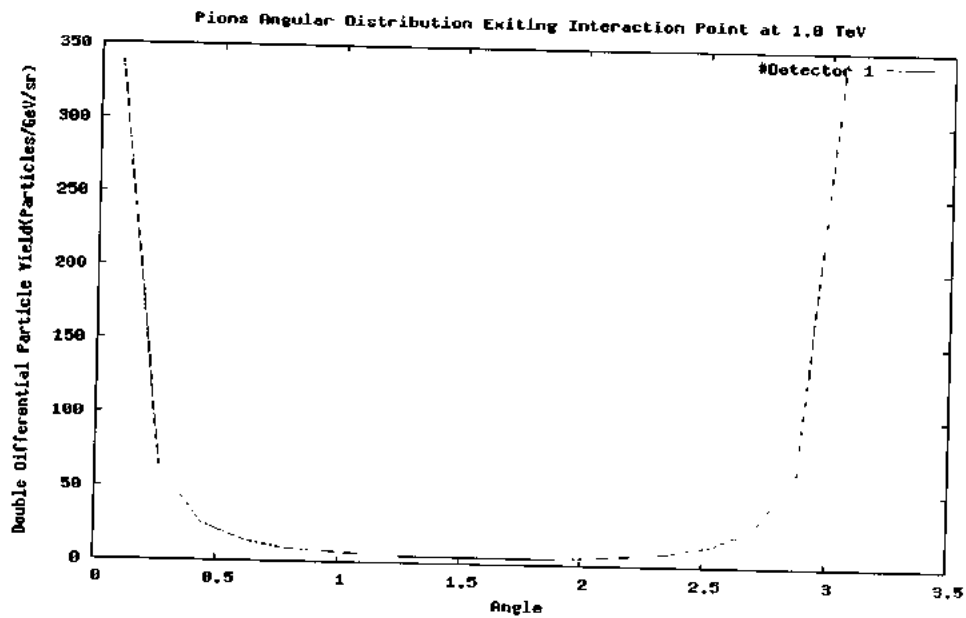Pions Angular Distribution Exiting Interaction Point at 1.0 TeV

Figure 4.21   Angular Distribution of Pions at 0.5 TeV.

Figure 4.22   Angular Distribution of Pions at 1.5 TeV.

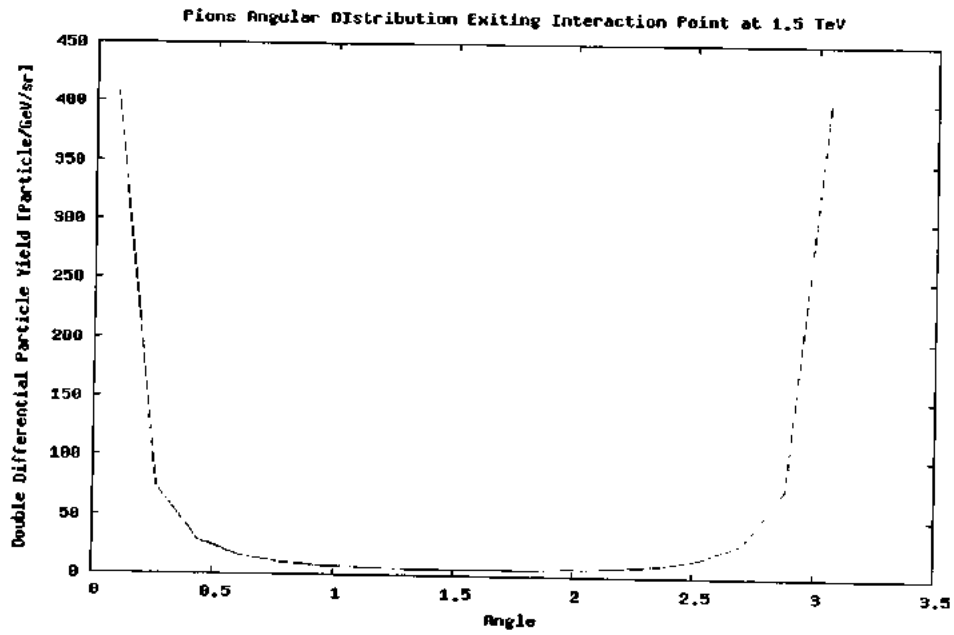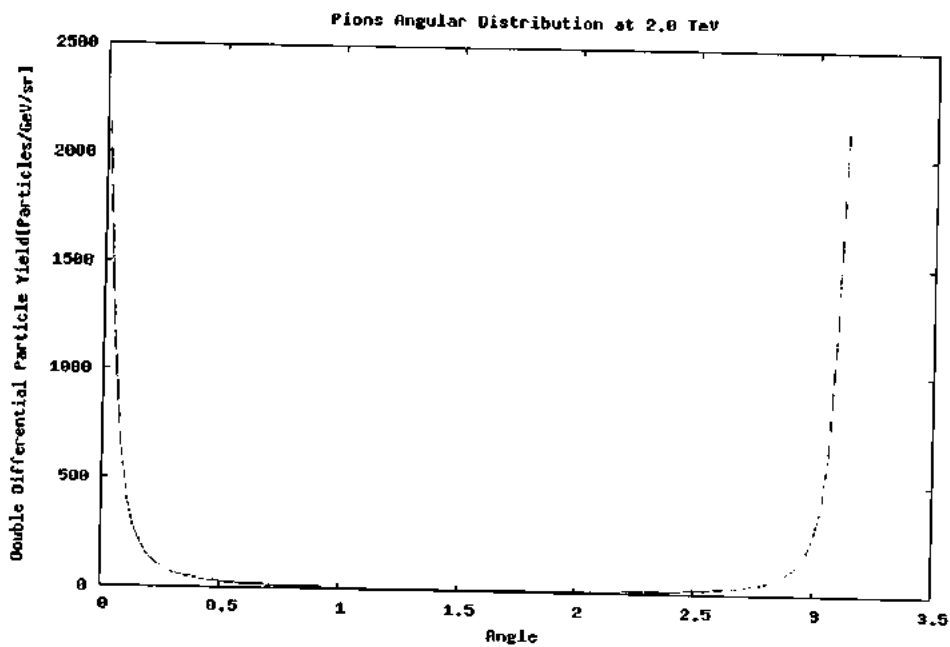Pions Angular Distribution at 2.0 TeV

Figure 4.23   Angular distribution of Pions at 2.0 TeV.

Figure 4.20 to Figure 4.23 are showing the angular distribution of Pions at 0.5 TeV, 1.0 TeV, 1.5 TeV and 2.0 TeV respectively. In these graphs the double differential fluence is taken along y-axis and angle is taken along x-axis. It is observed that large number of particles have been produced at the angle between 0 to 0.5 and 2.5 to 3.0, while the less number of particles have been observed at the other angles. Through studying these graphs one can concluded the ratio of produced particles at the angle between 2.5 to 3.0 is greater than that of 0 to 0.5 moreover the ratio of produced particles is increased by increasing beam energy.

4.7 CONCLUSIONS AND FUTURE RECOMMENDATIONS

In this research project the production of pions in Pb-Pb collisions at ultra-relativistic energies has been studied. It is observed that, at these energies enormous numbers of particles are produced with varying properties. In the present research work, double differential flounce count spectrums of pions is observed and analyzed which is a result of Pb-Pb collisions and this spectrum is acquired by using simulations of FLUKA software. The measurement for the single and double differential cross-sections with respect to energy and angle are also been executed. As a result of this study, it is concluded that flounce of the produced pions decreases with increase in the kinetic energy of the secondary particles. The particle's double differential count has an inverse relation with the secondary particle production. The reason of this inverse relation is decay of pi mesons into the secondary particle. Note that this relation of double differential count and primary energy is direct and linear.

In the extension of this work in future, one can measure the production cross sections of pions and other charged particles produced in Pb-Pb collisions at very high energies. The behavior of these charged particles at different angles can also be separately studied. It is also possible to test out the performance of pions and other particles as a function of mass instead of energy.

4.8 SUMMARY

Large Hadron Collider (LHC) at CERN is the world's biggest particle accelerator. The presented study is based on one of the LHC detector called ALICE which is a general purpose detector but particularly deliberated to study the heavy ion collisions and to observe a state of matter known as QGP. This phase of matter is supposed to be present in the early universe, about 10^{-5} second after the Big Bang. In this research work, production of pions in Pb-Pb collisions at various high energies has been studied, using Monte Carlo simulation package FLUKA, it is the latest Monte Carlo code which provides very precise simulations. The simulation is carried out by using FLUKA software to make energy spectrums of pions at several energy levels. Through studying these energy spectrums, it is observed that huge numbers of particles are produced as a result Pb-Pb interactions. The results achieved are then discussed which shows that the production of pions and other charged particles in Pb-Pb collisions at various collision energies can be fine understood in the presented study. These results explicitly show that, large numbers of pions are produced in very high kinetic energy range and the yield of pions decreases with increase in kinetic energy. As we move further along the x-axis, kinetic energy of daughter particles increases.

REFERENCES

1. H. Yukawa Rep. Physics Mathematical SO. Japan 17,(1993)

2. C.F. Powell, Rep Prog. Phys. 13(1950).

3. K. Aamodtet. el.,JINST 3, S08002 (2008).

4. JB Alessandro Et al, JINST 5, P02008 (2010).

5. http://www.lhc-closer.es/1/3/14/0

6. R Burn F.Cerminati, S.Giani , CERN-W5013.

7. Riazzudin "Charged Radius of Pion". Phys. Rev 114(4). 1184-1186 (1959).

8. K Nakamura *et al*, Nuclear and Particle Physics, Journal of Physics G, Volume 37-Number 7 A July (2010) Article075021

9. K.Warner Phys. Rep., 87 232(1993).

10. www.symmetrymagazine.org

11. http://hep.itp.tuwien.ac.at/~ipp/qgp.html

12. The Indian Lattice Gauge Theory Initiative

13. http://www.seslisozluk.net/search/particle+accelerator

14. P. J. Bryant. "A brief history and review of accelerators", CERN, Geneva, Switzerland

15. "What is LHCb". CERN FAQ. CERN Communication Group. January 2008. p. 44. http://cdsmedia.cern.ch/img/CERN-Brochure-2008-001-Eng.pdf. Retrieved 2010-04-02.

16. Amina Khan (31 March 2010). "Large Hadron Collider rewards scientists watching at Caltech". Los Angeles Times. http://articles.latimes.com/2010/mar/31/science/la-sci-hadron31-2010mar31. Retrieved 2010-04-02.

17. Roger Highfield (16 September 2008). "Large Hadron Collider: Thirteen ways to change the world"www.telegraph.co.uk/earth/main.jhtml?xml=/earth/2008/09/16/sciwriters116.xml. Retrieved 2008-10-10."Ions for LHC (I-LHC) Project". CERN. 1 November 2007. http://project-i-lhc.web.cern.ch/project-i-lhc/Welcome.htm. Retrieved 2009-04-17.

18. "Ions for LHC (I-LHC) Project". CERN. 1 November 2007. http://project-i-lhc.web.cern.ch/project-i-lhc/Welcome.htm. Retrieved 2009-04-17.

19. Paul Rincon (10 September 2008). "'Big Bang' experiment starts well". BBC News. http://news.bbc.co.uk/1/hi/sci/tech/7604293.stm. Retrieved 2009-04-17.

20. H. Yukawa, Rep. Physics-Mathematical SO. Japan 17, (1935).

21. http://hyperphysics.phy-astr.gsu.edu/hbase/quantum/fermi2.html

22. H. Yukawa, Rep. Physics-Mathematical SO. Japan **17**, (1935).

23. E.R. Jones and R.L. Childers Ed., Contemporary College Physics, Anderson Wesley Publishing Co. New York (1990) 915.

24. C.F. Powell, Rep. Prog. Phys., **13** (1950)

25. . D. Ashery and G.P. Schifler, Annu. Rev. Nucl. Sci., (1986) 207.

26. H.A. Khan, N.A. Khan and R.J. Peterson,Phys. Rev., **C35**, (1987) 645.

27. Nuclear and Particle Physics, Journals of Physics G, Volume 37-Number 7A July 2010, Article 075021

28. D.S. Ayres et al., Phys. Rev., **D3**, (1971) 1051.

29. The Indian Lattice Gauge Theory Initiative

30. Browman et al.,PhysRev. Lett., **33**, (1974) 1400.

31. M. Daum et al., Phys. Rev., **D20**, (1979) 2692.

32. http://th.physik.uni-frankfurt.de/~svogel/lecture_ss_2014/paper_5.pdf

33. LaszaloP.Csenai (2008) Introduction To Relativistic Heavy Ion Collisions,19-21

34. http://home.web.cern.ch/topics/large-hadron-collider

35. http://www.manuelsweb.com/temp.htm

36. ALICE section on US/LHC Website.

37. ALICE photography panorama.

38. Photography panorama of ALICE detector center.

39. http://public.web.cern.ch/Public/en/LHC/ALICE-en.html.

40. J. Alme et al.,Nucl. Instrum. Meth. A622 (2010) 316-367. [arXiv:1001.1950[physics.insdet]].

41. The ALICE Collaboration J. Instrum. 3 S08002 (2008).

42. The Alice Collaboration, ALICE Inner Tracking System (ITS): Technical Design Report(CERN, Geneva, 1999). 30

43. The ALICE Collaboration CERN-LHCC-99-012.

44. The ALICE Collaboration CERN-LHCC-2000-012.

45. ALICE collaboration, ALICE electromagnetic calorimeter: addendum to the ALICE technical proposal, CERN-LHCC-2006-014, http://cdsweb.cern.ch/record/932676

46. F. Carminati et al., ALICE: physics performance report, volume I, J. Phys. G 30 (2004)

47. The ALICE Collaboration, in Journal of Physics G: Nuclear and Particle Physics,eds.F.Carminati et al. (Institute Of Physics Publishing, (2004) p. 1517, doi:10.1088/0954-3899/30/11/001.

48. Aamodt K., et al.2008 The ALICE experiment at the CERN LHC J. Instrum. 3 S0800. 31

49. Aamodt K., et al.2008 The ALICE experiment at the CERN LHC J. Instrum. 3 S0800.

50. The Alice Collaboration, ALICE Dimuon Forward Spectrometer: Technical Design ReportCERN, Geneva, 1999).

51. D.V.Aleksandrov et.al., Nucl.Instrum.Methods A550,169-184 (2005)

52. A. Rashevsky et al.,Nucl. Instr. and Meth. A461 (2001) 133-138.

53. http://wwwinfo.cern.ch/asd/paw/

54. R. Brun, F. Bruyant, M. Maire, A.C. McPherson, P. Zanarini, CERN DD/EE/84-1, 1985.

55. Anderson, H.L. (1986). "Metropolis, Monte Carlo and the MANIAC". Los Alamos Science14: 96–108. http://library.lanl.gov/cgi-bin/getfile?00326886.pdf

56. Berg, Bernd A. (2004). Markov Chain Monte Carlo Simulations and Their Statistical Analysis (With Web-Based Fortran Code). Hackensack, NJ: World Scientific. ISBN 981-238-935-0.

57. Baeurle, Stephan A. (2009). "Multiscalemodeling of polymer materials using field-theoretic methodologies: A survey about recent developments". Journal of Mathematical Chemistry46 (2): 363–426. DOI:10.1007/s10910-008-9467-3.

58. Hubbard, Douglas (2007). How to Measure Anything: Finding the Value of Intangibles in Business. John Wiley & Sons. p. 46.

59. Hubbard, Douglas (2009). The Failure of Risk Management: Why It's Broken and How to Fix It. John Wiley & Sons.

60. http://AliSoft.cern.ch/offline/

61. A. Potrich, P. Tonella, C++ Code Analysis: an Open Architecture for the Verification of Coding Rules. Proceedings of the CHEP 2000. Padova, February 2000, p.758.

62. H.-U. Bengtsson, T. Sjostrand, Comput. Phys. Commun. 46 (1987) 43.

63. G. Marchesini, et al., Comput. Phys. Commun. 67 (1992) 465.

64. M. Gyulassy, X.N. Wang, Comput. Phys. Commun. 83 (1994) 307.

65. Ferrari, A., Fasso`, A., Ranft, J., Sala, P.R.: FLUKA: a multi-particle transport code, CERN 2005-10 (2005), INFN/TC_05/11, SLAC-R-773

66. G. Battistoni et al., FLUKA as a new high Energy cosmic ray generator, Nuclear Instruments and Methods in Physics Research A626-627 (2011) S191.

67. https://www.fluka.org/free_download/course/heidelberg2011/Lectures/Scoring031 1.pdf

68. https://www.google.com.pk/url?sa=t&rct=j&q=&esrc=s&source=web&cd=1&ved =0CBsQFjAAahUKEwjKv8v2s5PGAhUD6xQKHSbzAN8&url=https%3A%2F% 2Fwww.fluka.org%2Ffree_download%2Fcourse%2Fheidelberg2011%2FLectures %2FScoring0311.pdf&ei=8Kl_VcqHIoPWU6bmg_gN&usg=AFQjCNFt6d-Npn56YDpKzl5RdoqYoYGuUg&bvm=bv.96041959,d.d24&cad=rja.